Coherent Exciton-Phonon Dynamics in Organic Photovoltaics

I. Burghardt

Institute for Physical and Theoretical Chemistry, Goethe University Frankfurt, Germany

Thomas Young Centre
TYC Soirée – Excitons in Molecular Materials
London, 31st January 2019

Topics

1. Photoinduced Energy & Charge Transfer in Functional Organic Materials
    - Goal: First-Principles Approach to Organic Photovoltaics
    - Electron-Hole Lattice Models & Vibronic Coupling
    - Quantum Dynamics in Many Dimensions

Topics

1. Photoinduced Energy & Charge Transfer in Functional Organic Materials
   - Goal: First-Principles Approach to Organic Photovoltaics
   - Electron-Hole Lattice Models & Vibronic Coupling
   - Quantum Dynamics in Many Dimensions
2. Case Studies I: Exciton Migration Guided by Conformational Dynamics
   - Torsion-Induced Intra-Chain Exciton Migration
   - Ultrafast, Coherent Exciton-Polaron Dynamics
   - Temperature Effects: Ehrenfest-Langevin Dynamics

Topics

1. Photoinduced Energy & Charge Transfer in Functional Organic Materials
    - Goal: First-Principles Approach to Organic Photovoltaics
    - Electron-Hole Lattice Models & Vibronic Coupling
    - Quantum Dynamics in Many Dimensions

2. Case Studies I: Exciton Migration Guided by Conformational Dynamics
    - Torsion-Induced Intra-Chain Exciton Migration
    - Ultrafast, Coherent Exciton-Polaron Dynamics
    - Temperature Effects: Ehrenfest-Langevin Dynamics

3. Case Studies II: Exciton Break-Up at Donor-Acceptor Junctions
    - Oligothiophene-Fullerene (P3HT:PCBM Type) Junctions
    - Charge Transfer Excitons in Neat Polythiophene
    - Charge Transfer Excitons and Interfacial Charge Separation

OPV: Not Yet Competitive . . . But Making Progress!

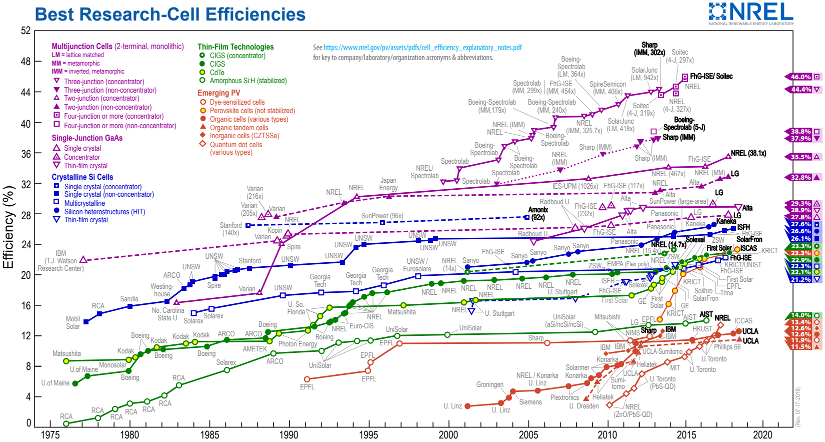

http://www.nrel.gov/ncpv/ (National Center for Photovoltaics)

- OPV: low-cost, large-area, flexible devices; superior low-light and high-temperature performance as compared with standard devices

Role of Electron-Phonon Coupling in Organic Photovoltaics

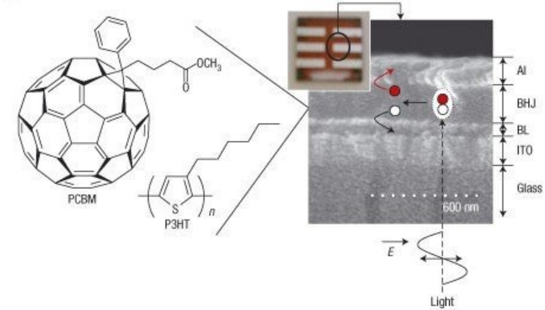

Kim et al., Nature Materials, 5, 197 (2006)

elementary steps:

- creation of electron-hole pairs (excitons)
- exciton migration to donor-acceptor interface area
- exciton dissociation at donor-acceptor junctions (here, PCBM-P3HT)[1]
- capture of charge carriers at electrodes
- potentially competing process: electron-hole recombination

---

[1] PCBM = phenyl-C_{61}-butyric acid methyl ester, P3HT = poly(3-hexylthiophene)

Zeroth-Order Picture of Donor/Acceptor Heterojunction

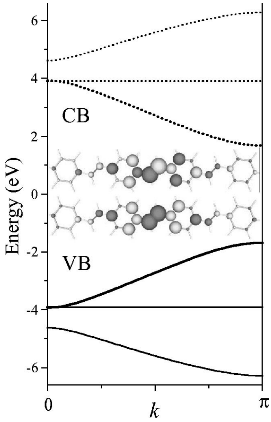

Karabunarliev & Bittner, J. Chem. Phys. **118**, 4291 (2003)

polymer/polymer interface:

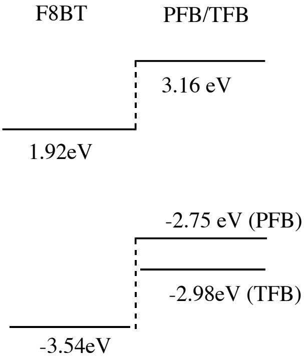

- HOMO/LUMO ↔ valence/conduction band
- 1st bound excited state: singlet exciton (${}^1B_u^-$ in PPV); Frenkel type exciton
- @junction: compare band offset vs. exciton binding energy ($\varepsilon_B \sim 0.5$ eV)

Exciton Dissociation at Bulk Heterojunctions (BHJ's)

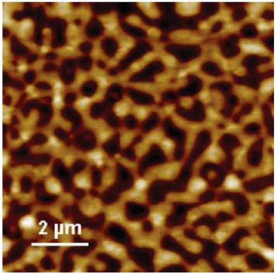

AFM image of d-F8:F8BT blend

McNeill & Greenham, Adv. Mater. 21, 1 (2009)

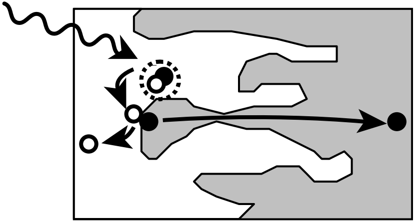

Schematic of exciton dissociation

Peumans, Uchida, Forrest, Nature **125**, 8098 (2003)

- bulk heterojunction technology led to breakthrough in ∼ 1995
- maximization of interface area ⟶ increase likelihood that excitons encounter interface within diffusion length ∼ 10 nm

What is the Best Nano-Morphology?

Highly ordered nanostructured domains (typically sub-10 nm) are thought to

- facilitate exciton diffusion
- favor exciton dissociation
- facilitate free carrier transport

Nanostructured domains can be achieved by

- self-assembly properties of D/A oligomers
- thin film processing methods (e.g., nanoimprint lithography)

However, the role of nanoscale ordering is controversial:

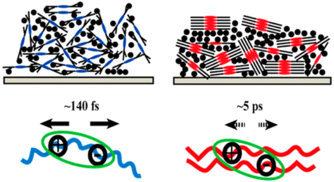

Guo et al., JACS 136, 10024 (2014)

- e.g., in a recent study of DA copolymer:fullerene systems, it is shown that the charge separation energetics changes unfavorably upon formation of crystalline domains

Insights from Spectroscopy

absorption spectrum: regioregular P3HT
with admixtures from regiorandom P3HT

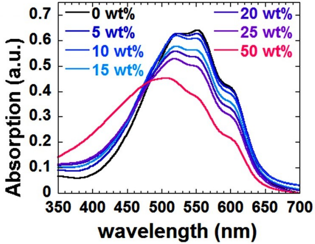

Vohra et al., Appl. Phys. Lett. (2012)

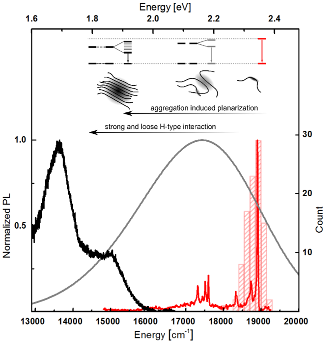

Raithel et al., Macromolecules 49, 9553 (2016)

- P3HT: inhomogeneous broadening across 200 nm
- huge red shift between solution and bulk: ordered low-energy conformations
- signatures of vibronic structure due to high-frequency modes ($\sim$1500 cm^{-1})
- single-molecule spectroscopy (here, @1.5K) unravels chromophore ensembles

Raithel et al., Macromolecules 49, 9553 (2016), Thiessen, Vogelsang, Adachi, Steiner, Vanden Bout, Lupton, PNAS E3550 (2013)

Time-Resolved Spectroscopies

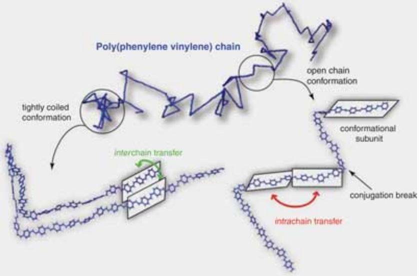

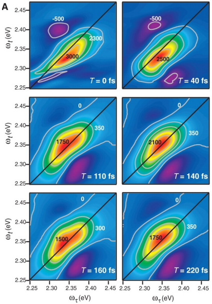

Collini, Scholes, Science 323, 369 (2009)

- 2D electronic spectroscopy monitors ultrafast energy and charge transfer

  Anna, Song, Dinshaw, Scholes, Pure. Appl. Chem. 85, 1307 (2013)

  De Sio, Lienau, PCCP 19, 18813 (2017)

- time-resolved Raman spectroscopy provides signatures of ultrafast structural dynamics

  Zhou, Yu, Bragg, J. Phys. Chem. Lett. 6, 3496 (2015)

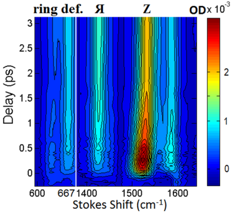

2D Electronic Spectroscopy of P3HT/PCBM Thin Films

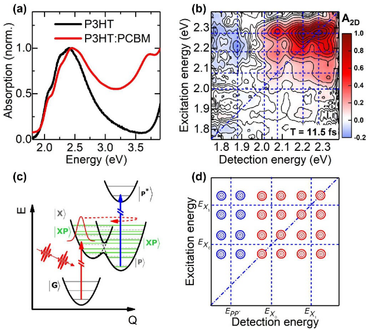

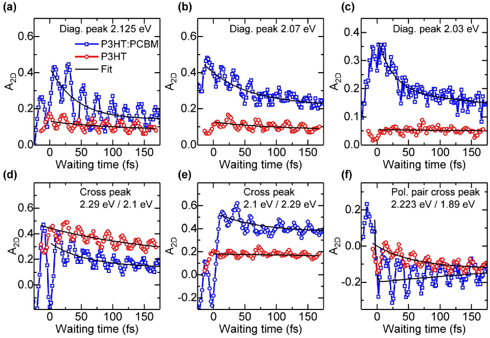

A. De Sio et al., Eur. Phys. J. B, 91, 236 (2018)

- 2D electronic spectroscopy of P3HT and P3HT/PCBM (Ch. Lienau & co)
- cross peaks reveal ultrafast transfer processes
- pronounced oscillatory signals
- long-lived vibrational/electronic/vibronic coherence?

Which Methods, Even for a Minimal Model?

- tens to hundreds of electronic states
- aggregate-type systems
- charge transfer and excitonic couplings$^{(*)}$ required
- delocalized excitations
- strong electron-phonon coupling
- non-Markovian dynamics
- non-exponential transfer
- coherent wavepacket dynamics
- standard rate theories (Förster / Marcus) not necessarily valid

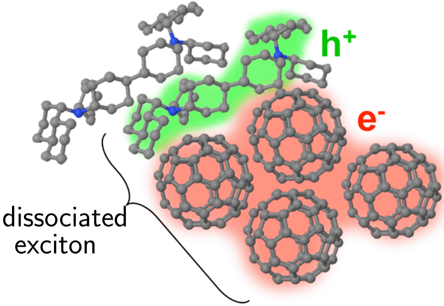

http://phys.org/news/2014-02-result-cheaper-efficient-solar-cells.html

$^{(*)}$excitonic coupling = transition density interaction:

$$V_{DA} = \frac{1}{4\pi\varepsilon_0} \int d\boldsymbol{r}_D\, d\boldsymbol{r}_A \frac{\rho_D^{(eg)}(\boldsymbol{r}_D)\,\rho_A^{(ge)}(\boldsymbol{r}_A)}{|\boldsymbol{r}_D - \boldsymbol{r}_A|} \longrightarrow \text{limiting case: transition dipole interaction}$$

Two Types of Approaches

approximate electron-nuclear dynamics:
e.g., time-dep. Kohn-Sham equation

$$i\frac{\partial}{\partial t}\varphi_i(r,t) = (-\frac{\nabla^2}{2} + v_{\mathrm{KS}}(r,t))\varphi_i(r,t)$$

expand in adiabatic KS basis,
$\varphi_i(r,t) = \sum_k c_{ik}(t)\tilde{\varphi}_k(r;R)$ such that

$$i\frac{dc_{ik}}{dt} = \sum_l c_{il}(t)(\varepsilon_l \delta_{kl} + d_{kl}\cdot\dot{R})$$

Ehrenfest or Surface Hopping dynamics
e.g., Craig, Duncan, Prezhdo, PRL 95, 163001 (2005)

pro's: no pre-computed potentials
con's: possibly poor description of excited states and nuclear dynamics

parametrized model Hamiltonian
+ multi-state quantum nuclear dynamics

$$i\frac{\partial}{\partial t}\psi(R,t) = \hat{H}\psi(R,t)$$

with a multi-state/site Hamiltonian

$$\hat{H} = \sum_{mn}(\hat{h}^{e}_{mn} + \hat{h}^{e\text{-}ph}_{mn}(R))|m\rangle\langle n| + \hat{H}^{ph}_0(R)$$

and $|\psi(R,t)\rangle = \sum_n c_n(t)\Phi_n(R,t)|n\rangle$

use (approximate) quantum dynamics
e.g., Kondov et al., JPCC 111 (2007), Tamura et al., JACS 135 (2013)

pro's: immediate physical interpretation
con's: restricted number of coordinates, electronic couplings *via* diabatization

Road Map: Model Hamiltonians & Quantum Dynamics

e-h lattice models + non-perturbative e-ph interaction + quantum dynamics

- electron-hole (e-h) lattice models including vibronic interactions
- *ab initio* (typically CC2, ADC(2)) and/or TD-DFT parametrization
- diabatization procedures to generate electronic couplings
- compute spectral densities and effective-mode decomposition
- efficient high-dimensional nonadiabatic quantum dynamics using multi-configurational methods (MCTDH) or reduced dynamics (HEOM) + semiclassical/quantum-classical approaches (SQC/MM, Ehrenfest)

- "molecular aggregate" perspective: parametrization for small fragments & dynamics for larger systems Polkehn, Eisenbrandt, Tamura, Burghardt, Int. J. Quant. Chem. 118:e25502 (2018)

CC2 = Second-Order Approximate Coupled-Cluster

ADC(2) = Second-Order Algebraic-Diagrammatic Construction (ADC(2)) scheme

MCTDH = Multi-Configuration Time-Dependent Hartree Beck et al., Phys. Rep. **324**, 1 (2000)

HEOM = Hierarchy of Equations of Motion Tanimura, J. Phys. Soc. Jpn. **75**, 082001 (2006)

Electron-Hole Lattice Model

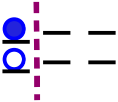

$|\mathbf{1_e}\rangle_C \otimes |\mathbf{1_h}\rangle_V$

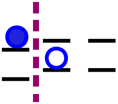

$|\mathbf{1_e}\rangle_C \otimes |\mathbf{2_h}\rangle_V$

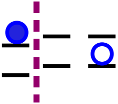

$|\mathbf{1_e}\rangle_C \otimes |\mathbf{3_h}\rangle_V$

- electron-hole (*e*-*h*) configurations: $|\mathbf{n}\rangle = |n_e n'_h\rangle = |n_e\rangle_C \otimes |n'_h\rangle_V$
- Hamiltonian in this basis:

$$\boxed{\hat{H} = \sum_{\mathbf{mn}} (\hat{h}^{eh}_{\mathbf{mn}} + \hat{h}^{eh\text{-}ph}_{\mathbf{mn}}(\mathbf{x})) |\mathbf{m}\rangle\langle\mathbf{n}| + \hat{H}^{ph}_0(\mathbf{x})}$$

Merrifield, J. Chem. Phys. 34, 1835 (1961)
Wang and Mukamel, Chem. Phys. Lett. 192, 417 (1992)
Karabunarliev and Bittner, J. Chem. Phys. 118, 4291 (2003)
Binder, Wahl, Römer, Burghardt, Faraday Discuss, 163, 205 (2013)

- includes Frenkel-type exciton (XT) states and charge transfer (CT) states
- oligomer (fragment) *ab initio* or TDDFT calc's: on-site energies, diabatic couplings
- vibronic couplings from Franck-Condon gradients, geometry optimization, PES cuts

Special Case: Frenkel Exciton Model

- Frenkel model ($n_e = n'_h = n$) often a good approximation to describe exciton
- exact analytic mapping of oligomer PES's to Frenkel model

Binder, Römer, Wahl, Burghardt, J. Chem. Phys. 141, 014101 (2014)

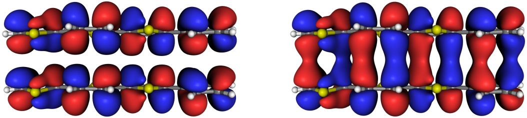

stacked oligothiophene $(\mathrm{OT4})_2$: "HJ aggregate"

- delocalized states
$$|\Psi_{\mathrm{exciton}}\rangle = \sum_{n}^{N_{\mathrm{exc}}} c_n |n\rangle$$
where $N_{\mathrm{exc}} \sim$ 5-10; $|n\rangle =$ configuration with single excitation on nth monomer
- trapping due to exciton-phonon interactions

- J-aggregate: end-to-end alignment of monomer units; lowest state of the exciton manifold is the bright state
- H-aggregate: plane-to-plane stacked geometry; highest state of the exciton manifold is the bright state
- HJ-aggregate: combination of both, as in stacked oligomers

Yamagata, Spano, JCP **136**, 184901 (2012)

HJ-Aggregate: Vibronic Lattice Model

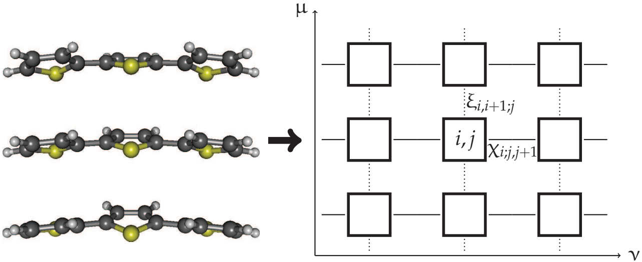

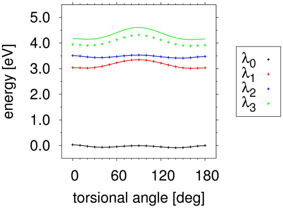

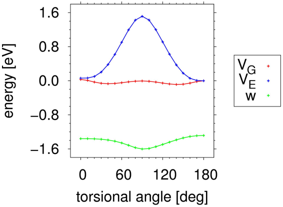

Binder, Römer, Wahl, Burghardt, J. Chem. Phys. 141, 014101 (2014)
Binder, Polkehn, Ma, Burghardt, Chem. Phys. 482, 16 (2017)

- here: analytic mapping of oligomer PES onto Hückel type model in 1D or 2D: solution to an inverse eigenvalue problem

  (NB.: V_G/V_E: monomer potentials, w: site-to-site coupling)

System-Bath Models

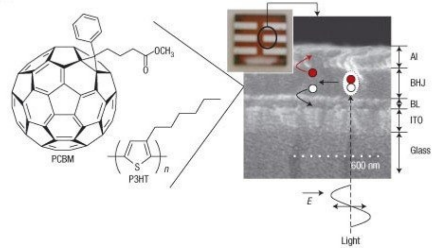

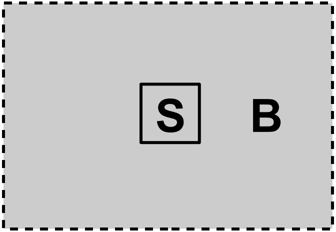

S region: e.g., electronic degrees of freedom (electron-hole states)

B region: all vibrations (phonons) mapped to harmonic oscillator model

$$\hat{H}_B + \hat{H}_{SB} = \sum_n \tfrac{1}{2}(\hat{p}_n^2 + \tfrac{1}{2}\omega_n^2 \hat{x}_n^2) + \hat{s}\sum_n c_n \hat{x}_n$$

$$\boxed{J(\omega) = \pi/2 \sum_n c_n^2/\omega_n \delta(\omega - \omega_n)}$$

spectral density

Spectral Densities from Electronic Structure Calculations$^{(*)}$

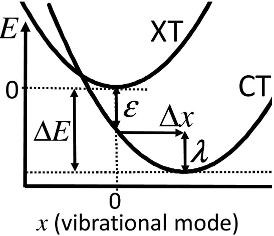

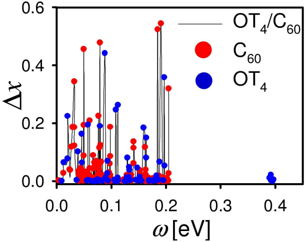

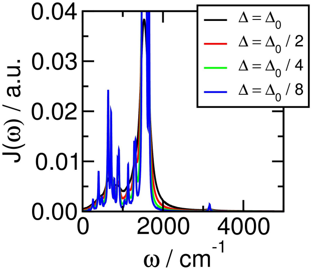

$$J(\omega) = \frac{\pi}{2} \sum_{n}^{N} \frac{c_n^2}{\omega_n} \delta(\omega - \omega_n) \simeq \frac{\pi}{2} \sum_{n}^{N} \frac{c_n^2}{\pi} \frac{\Delta}{(\omega - \omega_n)^2 + \Delta^2}$$

Tamura, Martinazzo, Ruckenbauer, Burghardt, J. Chem. Phys., 137, 22A540 (2012)

$^{(*)}$NB. Alternatively: obtain SD's from correlation functions (MD, CPMD, ...)

Bath Dynamics in Less Dimensions: Effective-Mode Chains

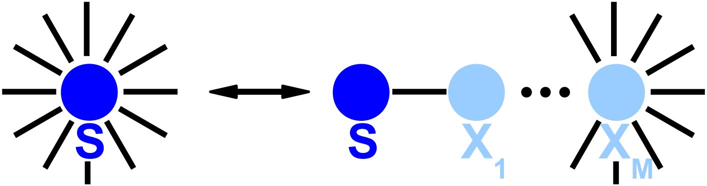

Martinazzo, Vacchini, Hughes, Burghardt, J. Chem. Phys. 134, 011101 (2011), Hughes, Christ, Burghardt, J. Chem. Phys. 131, 024109 (2009)
Tamura, Bittner, Burghardt, J. Chem. Phys. 126, 021103 (2007), Gindensperger, Köppel, Cederbaum, J. Chem. Phys. 126, 034106 (2007)
Cederbaum, Gindensperger, Burghardt, Phys. Rev. Lett., 94, 113003 (2005), Garg, Onucic, Ambegaokar, J. Chem. Phys. 83, 4491 (1985)

$$\boxed{\hat{H}_{SB} + \hat{H}_B = \hat{s} \sum_i c_n \hat{x}_n + \hat{H}_B \longrightarrow D \hat{s} \hat{X}_1 + d_{12} \hat{X}_1 \hat{X}_2 + \ldots + \hat{X}_M\text{–residual bath}}$$

- orthogonal coordinate transformation $\hat{X} = \mathbf{T}\hat{\boldsymbol{x}}$
- short-time dynamics captured by first few effective modes
- truncate hierarchical chain to define approximate, reduced-dimensional model
- (quasi-)Markovian closure
- connection to TD-DMRG!

Unitary Propagation vs. Master Equations

1. explicit, multidimensional dynamics for the full system + bath space: wavefunction $\psi_{SB}(t)$ or density operator $\hat{\rho}_{SB}(t) = \sum_n p_n |\psi_{n,SB}(t)\rangle\langle\psi_{n,SB}(t)|$

   ⟶ typically (ML-)MCTDH

   Meyer, Manthe, Cederbaum, Chem. Phys. Lett. **165**, 73 (1990), Beck et al., Phys. Rep. **324**, 1 (2000)

2. reduced dynamics (master equation) methods: $\hat{\rho}_S(t) = \mathrm{Tr}_B \hat{\rho}_{SB}(t)$

   ⟶ typically Hierarchy of Equations of Motion (HEOM)

   Tanimura, J. Phys. Soc. Jpn. **75**, 082001 (2006)

3. intermediate methods: explicit treatment of subsystem + effective-mode (E) part of the bath + master equation for residual (B') bath:[2]

$$\frac{\partial \hat{\rho}_{SE}}{\partial t} = -\frac{i}{\hbar}[\hat{H}_{SE}, \hat{\rho}_{SE}(t)] + \hat{\hat{L}}^{(B')}_{\mathrm{diss}} \hat{\rho}_{SE}(t) \quad ; \quad \hat{\rho}_{SE}(t) = \mathrm{Tr}_{\mathrm{B}'} \hat{\rho}_{SEB'}(t)$$

---

[2] e.g., Caldeira-Leggett: $\hat{\hat{L}}^{(B')}_{\mathrm{diss}} \hat{\rho}_{SE} = -i\frac{\gamma}{\hbar}[\hat{X}_E, [\hat{P}_E, \hat{\rho}_{SE}]_+] - \frac{2\gamma M k T}{\hbar^2}[\hat{X}_E, [\hat{X}_E, \hat{\rho}_{SE}]]$

Unitary Dynamics: MCTDH

$$\Psi(r,t) = \sum_{\nu} \sum_{J} A_{J,\nu}(t)\ \Phi_J(r,t)|\nu\rangle \equiv \sum_{\nu=1}^{N_{\text{el}}} \sum_{j_1=1}^{n_1} \cdots \sum_{j_N=1}^{n_N} A_{j_1\ldots j_N,\nu}(t) \prod_{\kappa=1}^{N} \varphi_{j_\kappa}^{(\kappa)}(r_\kappa,t)|\nu\rangle$$

- Multi-Configuration Time-Dependent Hartree: tensor approximation scheme
  Meyer, Manthe, Cederbaum, Chem. Phys. Lett. **165**, 73 (1990), Beck et al., Phys. Rep. **324**, 1 (2000)
- EoM's from the Dirac-Frenkel variational principle: $\langle \delta\Psi | \hat{H} - i\frac{\partial}{\partial t} | \Psi \rangle = 0$
- MCTDH takes one to 50-100 modes; exponential scaling alleviated
- restriction on the form of the potential: sums over products

- related multi-layer variant (ML-MCTDH) goes up to 1000 modes
  Wang, Thoss, J. Chem. Phys. 119, 1289 (2003), Manthe, J. Chem. Phys. 128, 164116 (2008), Vendrell, Meyer, *ibid* 134, 044135 (2011)
- related MCTDH-F (fermion) and MCTDH-B (boson) methods
  Kato, Kono, Chem. Phys. Lett. 392, 533 (2004), Nest, Klamroth, Saalfrank, J. Chem. Phys. 122, 124102 (2005)
  Alon, Streltsov, Cederbaum, Phys. Lett. A 362, 453 (2007)
- density matrix variant
  Raab, Burghardt, Meyer, J. Chem. Phys. 111, 8759 (1999)
- hybrid approaches: e.g., Gaussian-based variant (G-MCTDH, vMCG)
  Burghardt, Meyer, Cederbaum, J. Chem. Phys. 111, 2927 (1999), Worth, Burghardt, Chem. Phys. Lett. 368, 502 (2003)

Multi-Layer(ML)-MCTDH: Hierarchical Tensor Form

$$\Psi(r,t) = \sum_J A_J(t)\Phi_J(r,t) \;\; = \sum_J A_J(t) \prod_{\kappa=1}^{M} \varphi_{j_\kappa}^{(\kappa)}(r_\kappa, t)$$

where the 1st-layer SPFs $\varphi_{j_\kappa}^{(\kappa)}$ are now built as superpositions of 2nd-layer SPFs,

$$\varphi_{j_\kappa}^{(\kappa)}(r_\kappa,t) = \sum_L B_{j,L}^{(\kappa)}(t)\Phi_L^{(\kappa)}(r_\kappa,t) = \sum_L B_{j,L}^{(\kappa)}(t)\prod_\mu \varphi_{l_\mu}^{(\kappa,\mu)}(r_{\kappa_\mu},t)$$

. . . and so on . . .

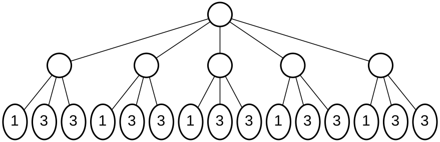

- repeated MCTDH scheme
- Mth order: ML-MCTDH
- "hierarchical Tucker format"
- recent Gaussian-based variant Römer, Ruckenbauer, Burghardt, J. Chem. Phys. 138, 064106 (2013)

Wang, Thoss, J. Chem. Phys. 119, 1289 (2003), Manthe, J. Chem. Phys. 128, 164116 (2008), Vendrell, Meyer, J. Chem. Phys. 134, 044135 (2011)

Objective: Capture Quantum Coherence Correctly

$$|\psi(t)\rangle = c_0(t)|0\rangle|\phi_0(t)\rangle + c_1(t)|1\rangle|\phi_1(t)\rangle$$

electronic coherence:

$$\rho_{01}(t) = \mathrm{Tr}[|0\rangle\langle 1|\hat{\rho}(t)] = \langle 1|\hat{\rho}(t)|0\rangle = c_1^*(t)c_0(t)\langle\phi_1(t)|\phi_0(t)\rangle$$

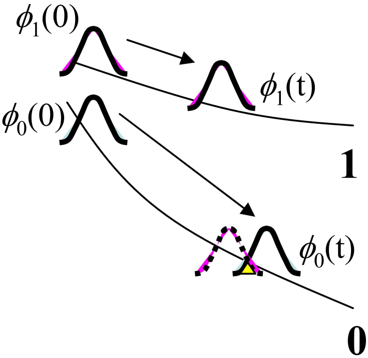

picture: P. Rossky et al.

- coherence $\propto$ overlap of nuclear wavefunctions
- typical decoherence times: tens to hundreds of fs or more (estimate from $\tau_{\mathrm{dec}} \sim \tau_g(6k_BT/\lambda)^{1/2}$ or $\tau_{\mathrm{dec}} \sim \gamma^{-1}(\lambda_T/\Delta x)^2$)

  Prezdho, Rossky, PRL 81, 5294 (1998)
- loss of coherence not captured by classical trajectory picture

Topics

Exciton Dynamics in Organic Semiconducting Polymers

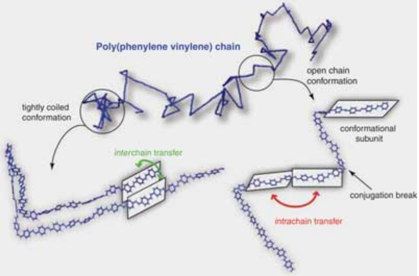

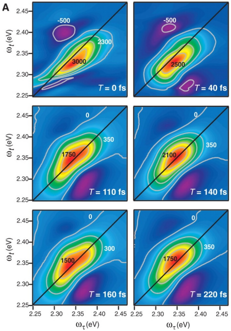

Collini, Scholes, Science 323, 369 (2009)

~0.1-1 ps: coherent intra-chain excitation energy transfer (EET) dynamics
~0.1-1 ps: self-trapped exciton-polaron states
~0.1-few ps: torsional geometry relaxation interfering with EET
~1-10 ps: inter-chain EET
~ps-ns: thermally assisted hopping

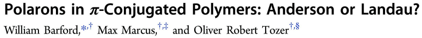

Polarons in π-Conjugated Polymers: Anderson or Landau?

William Barford,[*,†] Max Marcus,[†,‡] and Oliver Robert Tozer[†,§]

> *"We show that the high-frequency C-C bond oscillation only causes Landau polarons for a very narrow parameter regime; generally we expect disorder to dominate and Anderson polarons to be a more applicable description."*

J. Phys. Chem. A 120, 615 (2016)

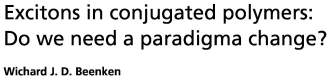

Excitons in conjugated polymers:
Do we need a paradigma change?

Wichard J. D. Beenken

> *"The fact that we could not find partition of excitons by structural defects – except of rare gauche defects and accidental chemical defects – leads us to the conclusion that we have to search for new mechanisms."*

Phys. Status Solidi A 206, 2750 (2009)

Does the Frenkel-Holstein Hamiltonian provide an answer?

$$\hat{H} = \sum_{n=1}^{N} \varepsilon_n \left|n\right\rangle \left\langle n\right| + \sum_{n=1}^{N-1} J(\left|n\right\rangle \left\langle n+1\right| + \left|n+1\right\rangle \left\langle n\right|) - \sqrt{2}\lambda\hbar\omega \sum_{n=1}^{N} q_n \left|n\right\rangle \left\langle n\right| + \frac{\hbar\omega}{2} \sum_{n=1}^{N} q_n^2$$

- nearest-neighbor excitonic interactions
- a single site-local mode per site
- shifted harmonic-oscillator potentials

Electronic Structure: Trapping in OPV Oligomers

Collaboration with H. Lischka, F. Plasser (Vienna/Texas Tech/Tianjin University)

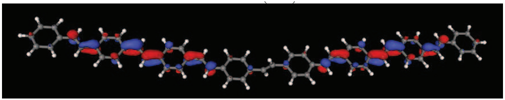

LUMO (105b)

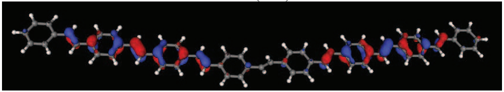

HOMO (106a)

- high-level electronic structure methods (ADC(2), CC2, MRCI)
- exciton trapping, due to BLA modes, described correctly

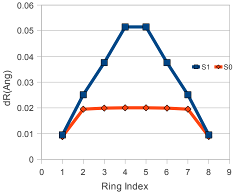

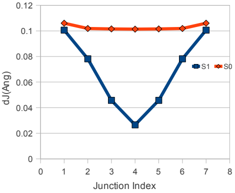

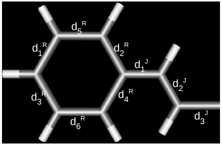

Panda, Plasser, Aquino, Burghardt, Lischka, JPCA, 117, 2181 (2013), see also: Sterpone, Rossky, JPCB 112, 4983 (2008), Nayyar et al., JPCL 2, 566 (2011)

Exciton Migration Guided by Conformational Dynamics

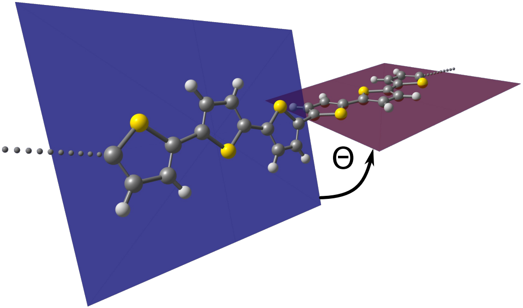

- full quantum dynamical study for small oligomers (5-20 units)
- Oligothiophene (OT) and Oligo-Phenylenevinylene (OPV)
- ML-MCTDH (up to 50 states, 100 vibrational modes)
- monomer-based, *ab initio* parametrized Hamiltonian

Binder, Wahl, Römer, Burghardt,
Faraday Discuss 163, 205 (2013)
Panda, Plasser, Aquino, Burghardt, Lischka
J. Phys. Chem. A, 117, 2181 (2013)
Wahl, Binder, Burghardt
Comp. Theor. Chem. 1040, 167 (2014)

- Is the transfer dynamics on ultrafast time scales coherent or of hopping type?
- Is a trapped exciton-polaron generated and if so, on which time scale?
- Is the spectroscopic unit concept valid?

see also: Tretiak, Saxena, Martin, Bishop, Conformational Dynamics of Photoexcited Conjugated Molecules, Phys. Rev. Lett. 89, 097402 (2002)

Dynamics: Test Case Oligothiophene OT-20

- Do we see trapped exciton-polarons in the dynamics?
- How exactly does the exciton migrate as the conjugation break "heals"?
- How does the spatial extension of the exciton change as a function of conformational (torsional) fluctuations?

Monomer representation:
most unbiased picture to answer these questions!

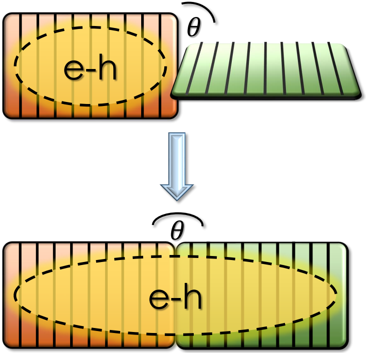

Relevant Coordinates: Torsions, CC Stretch, Ring Modes

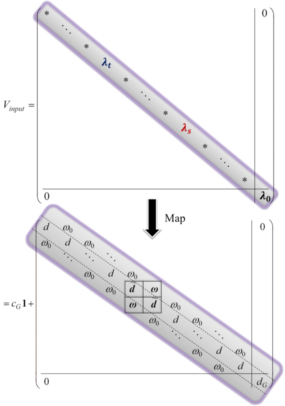

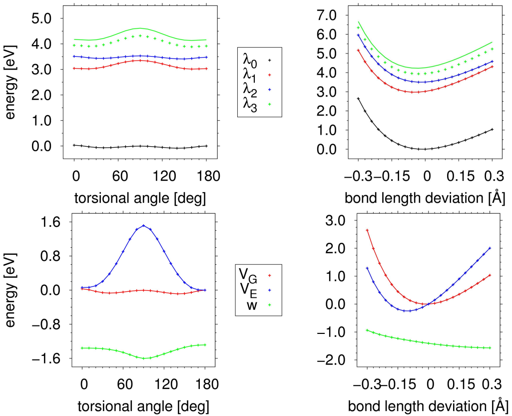

- analytical, pointwise mapping of oligomer PES's onto a Frenkel model
- diabatization in terms of solution to an inverse eigenvalue problem
- applicable to “extended Hückel systems” of J / H / HJ-aggregate type

Binder, Römer, Wahl, Burghardt, J. Chem. Phys., 141, 014101 (2014), Binder, Polkehn, Ma, Burghardt, Chem. Phys. 482, 16 (2017)

Ab initio Frenkel-Holstein Hamiltonian

$$\hat{H} \quad = \quad \sum_{n,n'=1}^{N} (\delta_{n,n'} \hat{T} + \delta_{n,n'} \hat{V}_n^{\text{site}} + \hat{V}_{n,n'}^{\text{exc}}) \left| n \right\rangle \left\langle n' \right| + \hat{H}_{\text{bath}} \hat{1}$$

- kinetic energy in curvilinear coordinates (using TNUM code):

$$\hat{T} = \frac{1}{2} \left(\sum_{n=1}^{N} G_{xx} \hat{p}_{x_n}^2 + \sum_{n=1}^{N-1} (G_{yy} \hat{p}_{y_{n,n+1}}^2 + G_{\theta\theta} \hat{p}_{\theta_{n,n+1}}^2) + 2 \sum_{n=1}^{N} G_{xy} \hat{p}_{x_n} (\hat{p}_{y_{n,n+1}} + \hat{p}_{y_{n,n-1}}) \right)$$

- site energies:

$$\hat{V}_n^{\text{site}}(\{\hat{x}, \hat{y}, \hat{\theta}\}) \quad = \quad \hat{V}_0(\{\hat{x}, \hat{y}, \hat{\theta}\}) + \hat{\Delta}_n(\hat{x}_n, \hat{y}_{n,n\pm1}, \hat{\theta}_{n,n\pm1})$$

with the difference potential

$$\hat{\Delta}_n(\hat{x}_n, \hat{y}_{n,n\pm1}, \hat{\theta}_{n,n\pm1}) \quad = \quad c_{\mathsf{E}} + \hat{v}_{\mathsf{E}} \left(\hat{x}_n, \hat{y}_{n,n\pm1}, \hat{\theta}_{n,n\pm1} \right) - \hat{v}_{\mathsf{G}} \left(\hat{x}_n, \hat{y}_{n,n\pm1}, \hat{\theta}_{n,n\pm1} \right)$$

- excitonic coupling:

$$\hat{V}_{n,n\pm1}^{\text{exc}}(\hat{\theta}_{n,n\pm1}) \quad = \quad \hat{w}(\hat{\theta}_{n,n\pm1}) \qquad \longleftarrow$$

large (of the order of 1 eV)

reduces to standard Frenkel-Holstein model if

- the excitonic coupling is constant
- a single *site-local* mode per site is included
- the monomer potentials conform to shifted harmonic-oscillator potentials

Relevant Coordinates: Torsions, CC Stretch, Ring Modes

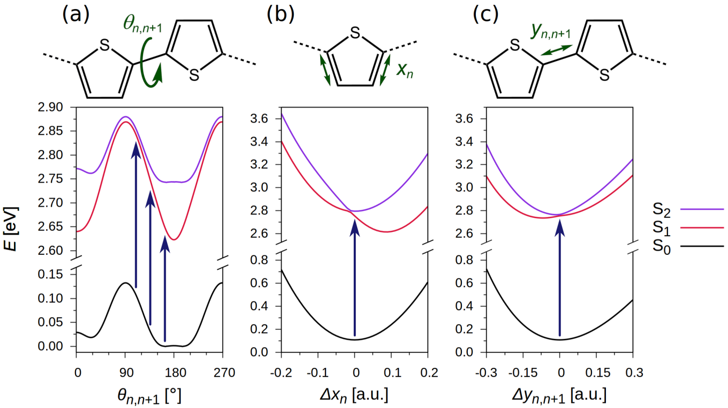

- high-dimensional PES as a function of site-local and site-correlated modes
- 20 monomer sites, 50 phonon modes

Quantum Dynamics: Hierarchical Multi-Layer MCTDH Tree

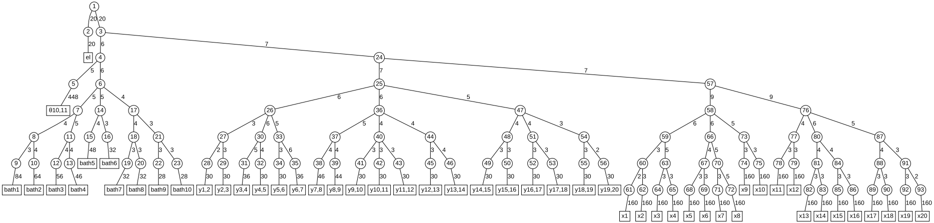

- ML-MCTDH (20 states, 50 modes)
- 7 layers, 2-10 single-particle functions (SPFs) – highly correlated system!
- combined electronic particle (here, 20 states)
- active torsional mode as isolated particle (long DVR grid)
- delocalized initial condition prepared by imaginary time propagation

Binder, Lauvergnat, Burghardt, Phys. Rev. Lett. 120, 227401 (2018), Supp. Mater.

Quantum Dynamics: 20-Site J-Aggregate with Central Torsion

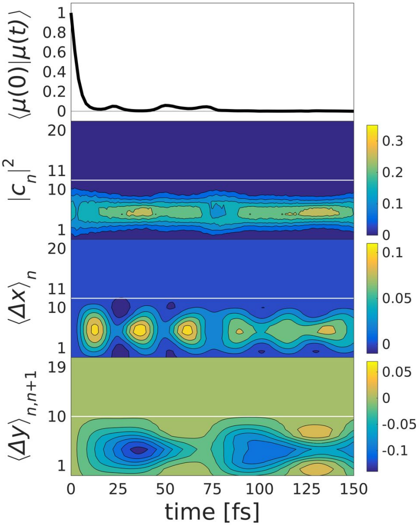

Binder, Lauvergnat, Burghardt, Phys. Rev. Lett. 120, 227401 (2018)

- ML-MCTDH calculations: 20 states, 50 modes (6-layer set-up)
- earliest time scale: exciton trapping (contraction by ∼3 sites)
- high-frequency modes adapt to exciton: quasi-stationary trapping
- LEGS = local exciton ground state: nodeless left-localized exciton

  Tozer, Barford, JPCA 116:10310 (2012)
- ultrafast decay of transition dipole autocorrelation function (∼10 fs): $\langle\mu(0)\mu(t)\rangle = |\mu|^2\langle\psi_{\rm exc}(0)|\psi_{\rm exc}(t)\rangle$
- relates to anisotropy decay: ∼40 fs

  Grage et al., Phys. Rev. B, 67, 205207 (2003)

Quantum Dynamics: 20-Site J-Aggregate with Central Torsion

C-C inter-monomer mode + local C=C + torsion + bath

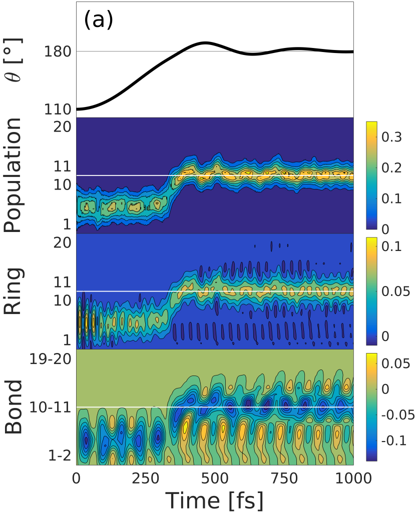

C-C inter-monomer + torsion + bath

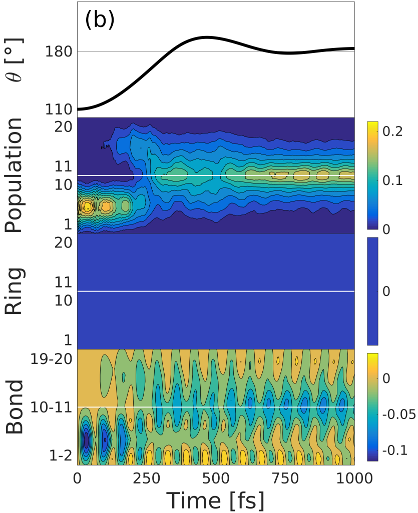

Electronic Structure – Torsion Dependence

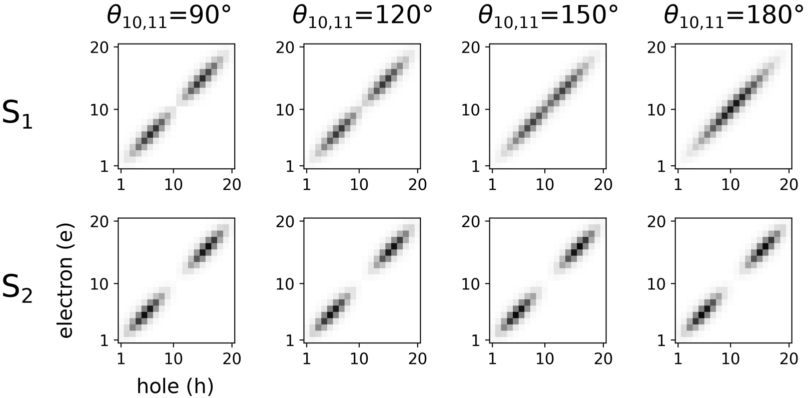

- transition density analysis

Panda, Plasser, Aquino, Burghardt, Lischka, JPCA (2013), Binder, Lauvergnat, Burghardt, Phys. Rev. Lett. 120, 227401 (2018)

- particle-in-the-box type e-h states
- marked dependence on torsion
- LEGS $=$ local exciton ground state: nodeless S_1 exciton @180°

Tozer, Barford, JPCA 116:10310 (2012)

Two Time-Scale Process

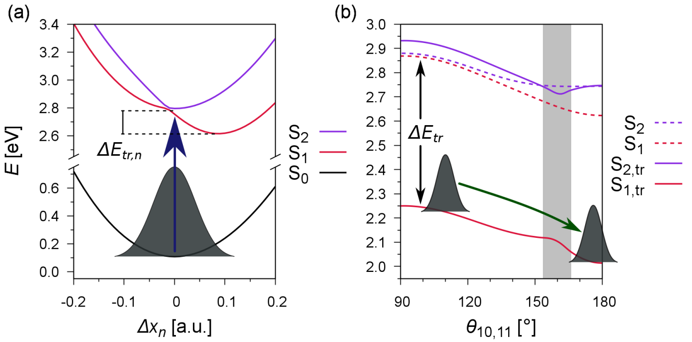

- dynamics is essentially happening on coupled S_1/S_2 surfaces
- effective torsion potentials including stabilization due to trapping $(S_{1,\mathrm{tr}}/S_{2,\mathrm{tr}})^1$
- initial left/right localized state = superposition of S_1/S_2
- energy loss due to external bath acting on torsional mode
- exciton-polaron: quasi-stationary trapping at all stages of the dynamics

---

[1] i.e., “polaron transformed” potentials

Binder, Lauvergnat, Burghardt, PRL 120, 227401 (2018)

Initial vs. Final States: Absorption Spectra

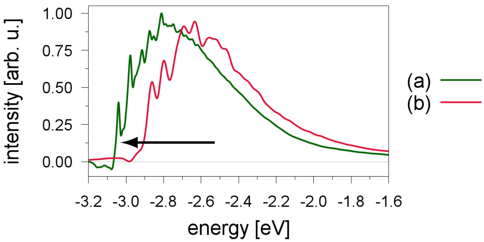

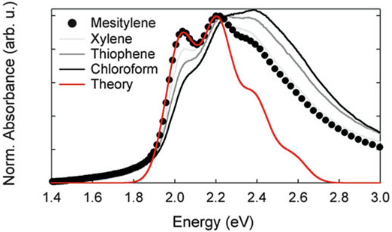

Tremel, Ludwigs, Adv. Polym. Sci. 265, 39 (2014)

- spectra calculated from Fourier transform of $C(t) = \langle \psi(0) | \psi(t) \rangle$:
  (a) full 20-mer system: torsionally relaxed, stationary state
  (b) left-localized 10-mer fragment for initial defect structure
  (a) $\longleftarrow$ (b): downhill energy transfer
- dominant vibronic signature of ring-breathing mode

Temperature Effects: Ehrenfest/Langevin dynamics

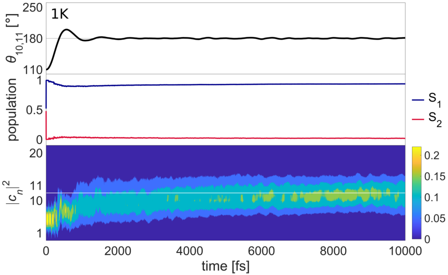

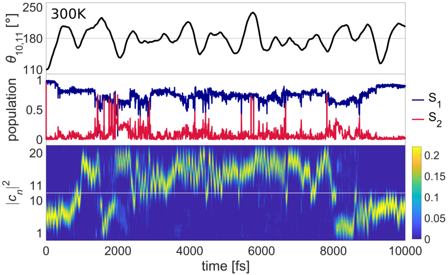

- single-trajectory simulation, with ZPE of high-frequency modes removed
- exciton migration at higher T is related to repeated non-adiabatic events
- interplay of torsional fluctuations and trapping explains observations
- quantum benchmark simulations needed (*via* random-phase wavefunctions, or thermofield method, combined with MCTDH)

Wahl, Hegger, Binder, Burghardt, in preparation

Exciton Migration: Ehrenfest/Langevin dynamics

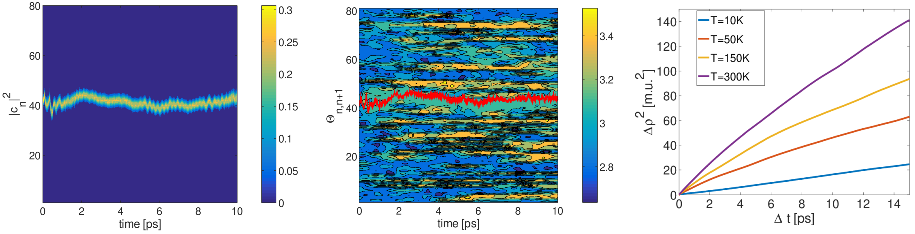

- single-trajectory simulation; 80-site lattice
- overdamped high-frequency modes, essentially confining the dynamics to S_1
- torsional fluctuations induce diffusive exciton-polaron dynamics
- channel of planarized torsions (green) along exciton path (red)
- mean-square displacement is near-linear: $\Delta\rho^2 \sim Dt$
- diffusion coefficient slightly larger than observed experimentally

Wahl, Hegger, Binder, Burghardt, in preparation

Polarons in π-Conjugated Polymers: Anderson or Landau?

William Barford,[*,†] Max Marcus,[†,‡] and Oliver Robert Tozer[†,§]

> *"We show that the high-frequency C-C bond oscillation only causes Landau polarons for a very narrow parameter regime; generally we expect disorder to dominate and Anderson polarons to be a more applicable description."*

J. Phys. Chem. A 120, 615 (2016)

Excitons in conjugated polymers: Do we need a paradigma change?

Wichard J. D. Beenken

> *"The fact that we could not find partition of excitons by structural defects – except of rare gauche defects and accidental chemical defects – leads us to the conclusion that we have to search for new mechanisms."*

Phys. Status Solidi A 206, 2750 (2009)

Our interpretation: Exciton-polarons driven by defects and fluctuations

- exciton-polaron species: "exciton dressed by a cloud of local oscillators"
- typical delocalization length: 5-10 units (in line with experiment)
- Landau polaron (or Holstein "large" polaron) subject to disorder
- torsional defects confine excitons to sublattices ("spectroscopic units")
- hopping-type transition between exciton-polaron states induced by torsion
- elementary step is coherent motion of the trapped exciton

Topics

1. Photoinduced Energy & Charge Transfer in Functional Organic Materials
   - Goal: First-Principles Approach to Organic Photovoltaics
   - Electron-Hole Lattice Models & Vibronic Coupling
   - Quantum Dynamics in Many Dimensions
2. Case Studies I: Exciton Migration Guided by Conformational Dynamics
   - Torsion-Induced Intra-Chain Exciton Migration
   - Ultrafast, Coherent Exciton-Polaron Dynamics
   - Temperature Effects: Ehrenfest-Langevin Dynamics
3. Case Studies II: Exciton Break-Up at Donor-Acceptor Junctions
   - Oligothiophene-Fullerene (P3HT:PCBM Type) Junctions
   - Charge Transfer Excitons in Neat Polythiophene
   - Charge Transfer Excitons and Interfacial Charge Separation

Oligothiophene-Fullerene Junctions

(collaboration with Hiroyuki Tamura (Sendai), Keith Hughes (Bangor), Rocco Martinazzo (Milano))

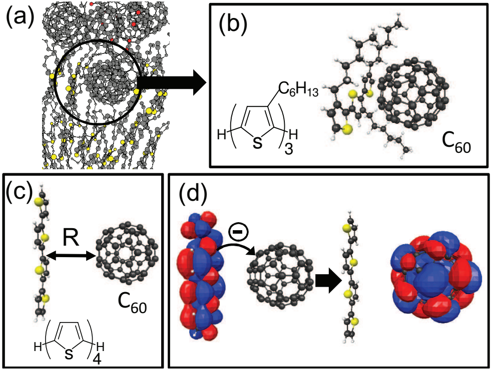

Tamura, Burghardt, Tsukada, JPCC, **115**, 10205 (2011)

- model for polymer-fullerene heterojunctions, e.g., P3HT-PCBM [2]
- ultrafast initial charge transfer ($\sim$ 50 fs [Brabec et al., CPL (2001)])
- but subsequent generation of free charge carriers not necessarily ultrafast

---

[2] PCBM = phenyl-C_{61}-butyric acid methyl ester, P3HT = poly(3-hexylthiophene)

Oligothiophene-Fullerene Junction: Dimer Model

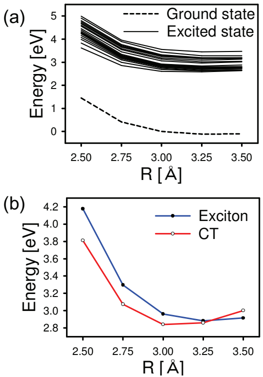

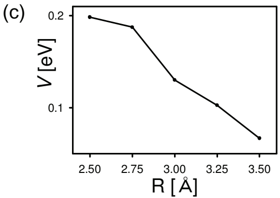

diabatic coupling: distance dependence

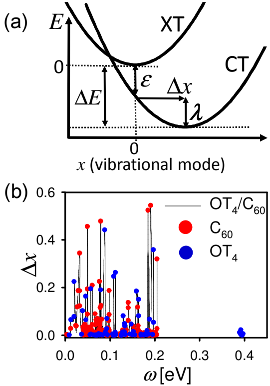

- LC-TDDFT calculations (LC = long-range corrected)
- diabatization scheme using reference functions of pure XT vs. CT character
- normal mode analysis for separate C_{60}^{-} and OT_4^{+} fragments (264 modes)

Tamura, Burghardt, Tsukada, J. Phys. Chem. C, 115, 10205 (2011)

Two-State XT-CT Charge Transfer Model

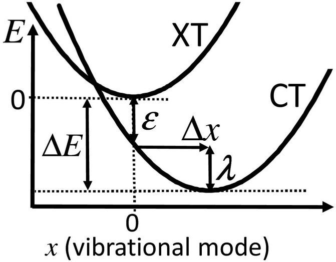

$$\boxed{\hat{H} = \hat{H}_0 + \hat{H}_R + \hat{H}_B}$$

$\hat{H}_0$: electronic part
$\hat{H}_R$: inter-fragment coordinate part
$\hat{H}_B$: phonon bath part

$$\hat{H}_0 = \Delta_{\mathrm{XT-CT}}|\mathrm{CT}\rangle\langle\mathrm{CT}| + \gamma\big(|\mathrm{XT}\rangle\langle\mathrm{CT}| + |\mathrm{CT}\rangle\langle\mathrm{XT}|\big)$$

$$\begin{aligned}\hat{H}_R \quad = \quad & \frac{\omega_R}{2}(\hat{R}^2 + \hat{P}^2) + \kappa_R \hat{R}\,|\mathrm{CT}\rangle\langle\mathrm{CT}| \\ & + \gamma_R \hat{R}\left(|\mathrm{XT}\rangle\langle\mathrm{CT}| + |\mathrm{CT}\rangle\langle\mathrm{XT}|\right)\end{aligned}$$

$$\hat{H}_B = \sum_{i=1}^{N} \frac{\omega_i}{2}(\hat{x}_i^2 + \hat{p}_i^2) + \sum_{i=1}^{N} \kappa_i x_i\,|\mathrm{CT}\rangle\langle\mathrm{CT}| + \sum_{i=1}^{N} \frac{\kappa_i^2}{2\omega_i}$$

Tamura, Martinazzo, Ruckenbauer, Burghardt, J. Chem. Phys., 137, 22A540 (2012)

Ultrafast Coherent Transfer Dynamics

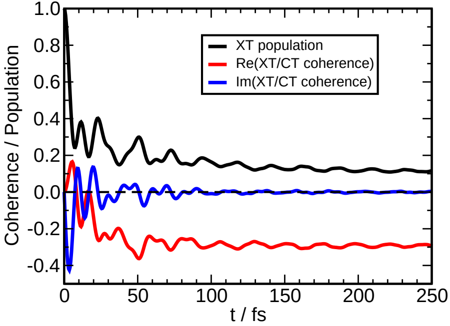

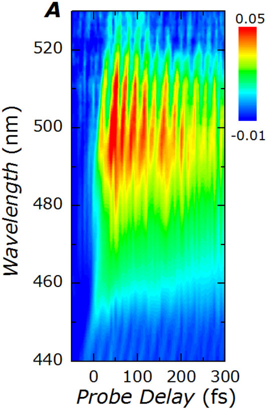

Falke, Rozzi, . . . , Lienau, Science, 344, 1001 (2014)

el. coherence: $\rho_{XT,CT}(t) = \mathrm{Tr}\left\{|\mathrm{CT}\rangle\langle\mathrm{XT}|\hat{\rho}(t)\right\}$

- imaginary part $(-2\gamma/\hbar)\mathrm{Im}\rho_{XT,CT}$ ↔ population flux
- real part ↔ stationary coherent superposition ($P_{\mathrm{XT}} \sim 0.1$, $P_{\mathrm{CT}} \sim 0.9$)
- experiment: ultrafast ET ($\sim$ 50 fs), oscillatory features [Brabec et al., CPL (2001)]) confirmed by recent pump-probe experiments by Lienau group [Science (2014)])

Temperature Dependence Not a Key Factor

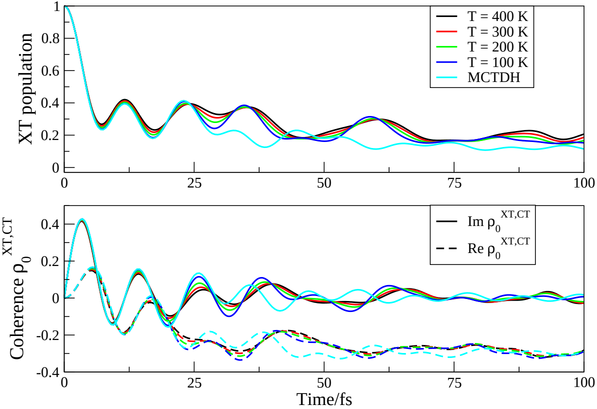

- Hierarchical Equations of Motion (HEOM) approach Tanimura, J. Phys. Soc. Jpn. **75**, 082001 (2006)
- reduced dynamics + effective mode decomposition Burghardt et al., JCP 137, 144107 (2012)
- experiments show negligible temperature dependence Pensack, Asbury, JACS 131, 15986 (2009)

Hughes, Cahier, Martinazzo, Burghardt, Chem. Phys., 442C, 111 (2014)

Marcus Theory Doesn't Work for Ultrafast Charge Transfer

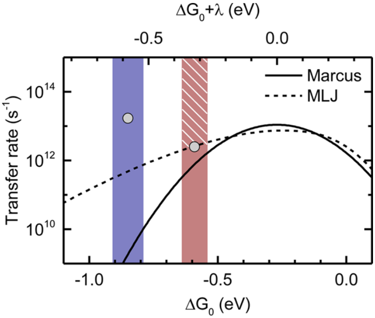

filled circles: experiments P3HT/PCBM
(blue: electron transfer, red: hole transfer)

Unger et al., J. Phys. Chem. C 121, 22739 (2017)

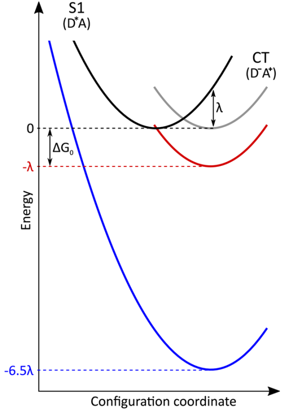

- Marcus (M) & Marcus-Levich-Jortner (MLJ) rates:

$$k_{\mathrm{M}} = \frac{|V|^2}{\hbar}\sqrt{\frac{\pi}{\lambda k_B T}}\exp\left[-\frac{(\lambda+\Delta G_0)^2}{4\lambda k_B T}\right] \quad ; \quad k_{\mathrm{MLJ}} = \frac{|V|^2}{\hbar}\sqrt{\frac{\pi}{\lambda_0 k_B T}}\sum_{\nu=0}^{\infty}\frac{e^{-S}S^{\nu}}{\nu!}\exp\left[-\frac{(\lambda+\Delta G_0)^2}{4\lambda k_B T}\right]$$

Free Carrier Generation

(collaboration with Hiroyuki Tamura (WPI-AIMR Tohoku University))

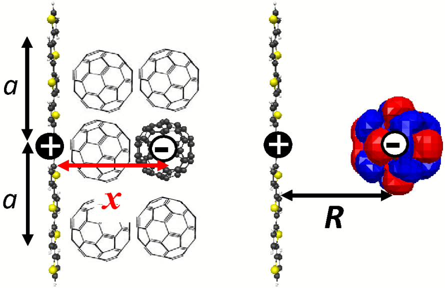

Tamura, Burghardt, JPCC, 117, 15020 (2013)

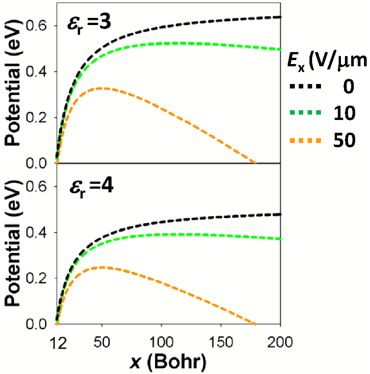

- Coulomb barrier to free carrier generation: suggests trapped interfacial state
- validity of Onsager-Braun rate model for CT break-up to be questioned
- "hot CT" hypothesis: efficient charge separation due to excess energy
- charge delocalization can lead to strong decrease of barrier

Interfacial Trapping vs. Long-Range Charge Separation

$$\begin{aligned}\hat{H} &= \hat{H}_{\mathrm{XT_1\text{-}CT}}(\mathbf{x}) + \sum_n \hat{H}^{(n)}_{\mathrm{CS}}(\mathbf{x})|\mathrm{CS}_n\rangle\langle\mathrm{CS}_n| + t(\mathbf{x})(|\mathrm{CS}_1\rangle\langle\mathrm{CT}| + \sum_{nn'}|\mathrm{CS}_n\rangle\langle\mathrm{CS}_{n'}| + h.c.)\\ &\quad + \sum \hat{H}^{(n)}_{\mathrm{XT}}(\mathbf{x})|\mathrm{XT}_n\rangle\langle\mathrm{XT}_n| + j(\mathbf{x})\sum(|\mathrm{XT}_n\rangle\langle\mathrm{XT}_{n'}| + h.c.)\end{aligned}$$

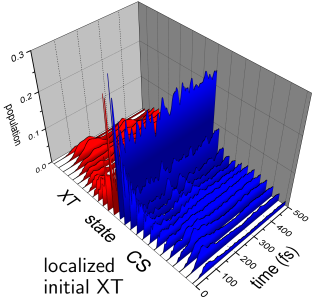

localized
initial XT

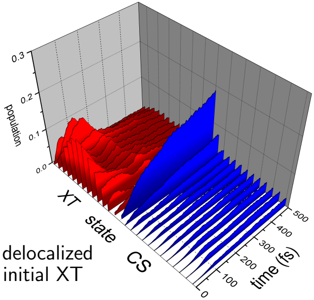

delocalized
initial XT

- CT/CS generation depends on exciton (de)localization
- ML-MCTDH calculations: 26 states/120 modes (barrier II)

Tamura, Burghardt, JACS (Communication) 135, 16364 (2013), Huix-Rotllant, Tamura, Burghardt, J. Phys. Chem. Lett. 6, 1702 (2015)

Electronic Eigenstate Picture

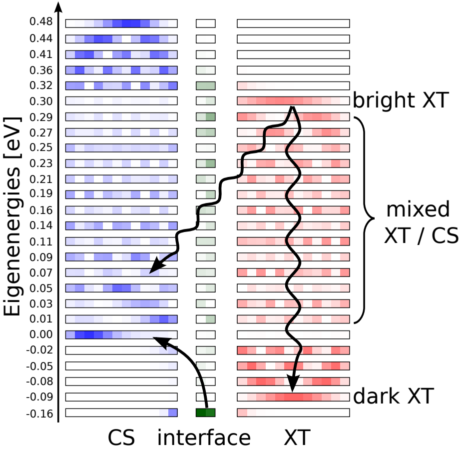

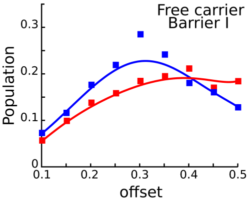

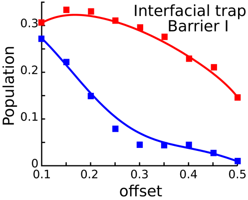

- interplay of delocalization, internal conversion, and charge transfer
- de/localized initial condition (blue/red) reduces/enhances interfacial trapping

Huix-Rotllant, Tamura, Burghardt, J. Phys. Chem. Lett., 6, 1702 (2015)

"Quantum Coherence Controls the Charge Separation in a Prototypical Organic Photovoltaic System"

Lienau and collaborators (Science, 2014)

- electronic/vibronic coherence on shortest time scales
- vibrational coherence (wavepacket motion): can persist longer
- delocalization enhances coherence
- static and dynamic disorder

- coherent vibronic effects and fluctuations far away from equilibrium
- very different picture from Marcus theory!

Charge Transfer Excitons in Neat Regioregular Polythiophene

experiment: Reid et al., Chem. Mater. 26, 561 (2014), De Sio et al., Nature Comm. 7, 13742 (2016)

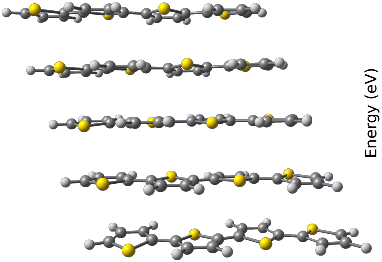

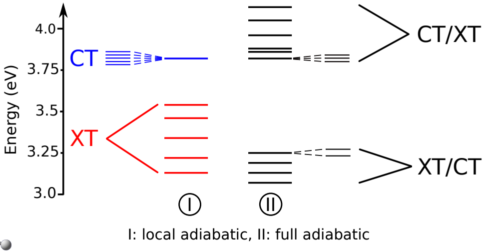

I: local adiabatic, II: full adiabatic

Popp, Polkehn, Tamura, Burghardt, to be submitted

- inter-chain CTX states favored in PT (as compared with, e.g., PPV)
- electronic structure (ADC(2), TDDFT): low-energy inter-chain CT states
- representative quantum dynamics calculations for $(\mathrm{OT})_n$, $n = 3, 5$
- diabatization + Linear Vibronic Coupling (LVC) model
- ML-MCTDH for up to 13 electronic states, 196 modes

Charge Transfer Excitons in Neat Regioregular Polythiophene

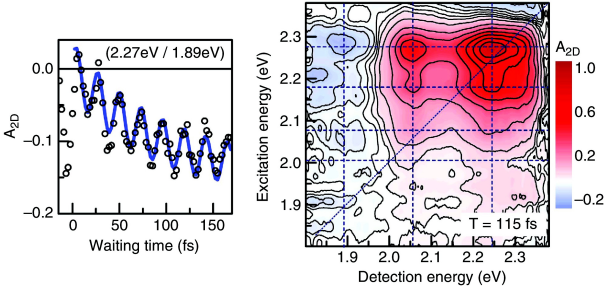

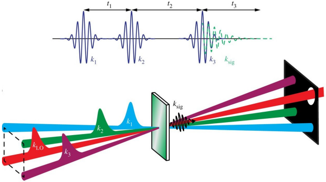

De Sio et al., Nature Comm. 7, 13742 (2016)

- 2D electronic spectroscopy of P3HT (thin film)
- polaron cross-peak signal assigned to inter-chain CTX states
- sustained high-frequency oscillations (23 fs periodicity)
- similar observations by Scholes & collaborators   Song et al., JCP 142, 212410 (2015)
- What is the origin of the persistent oscillations?

Photoexcitation to a Coherent XT/CTX Superposition State

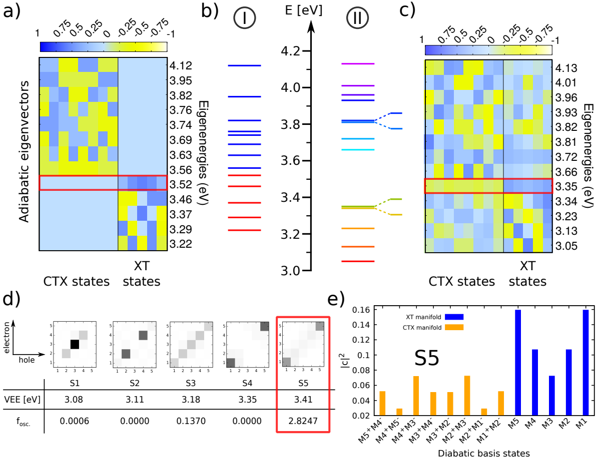

	S1	S2	S3	S4	S5
VEE [eV]	3.08	3.11	3.18	3.35	3.41
$f_{osc.}$	0.0006	0.0000	0.1370	0.0000	2.8247

Popp, Polkehn, Tamura, Burghardt, to be submitted (2018)

- bright state (S_5) looks distinctly different from typical H-aggregate (inverted curvature of nodeless exciton wavefunction) Hestand and Spano, J. Chem. Phys. 143, 244707 (2015)

Spectral Densities (SD's)

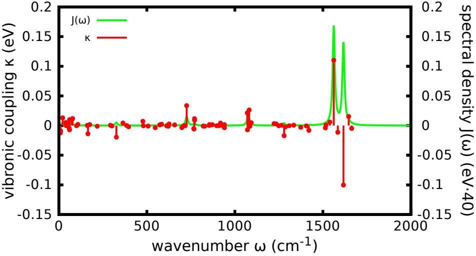

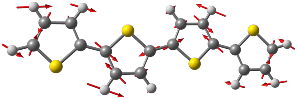

76
1562

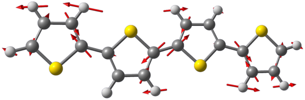

78
1617

- SD's calculated from state-specific Frank-Condon gradients
- SD's show large amplitude (∼ Huang-Rhys factor) for CC stretch modes
- SD's similar for various electronic states
- use SD's to parametrize Linear Vibronic Coupling (LVC) Hamiltonian
- ML-MCTDH: 13 states/196 modes (or 78 effective modes)

Effective Mode Reconstruction of SD

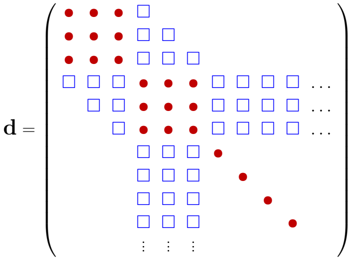

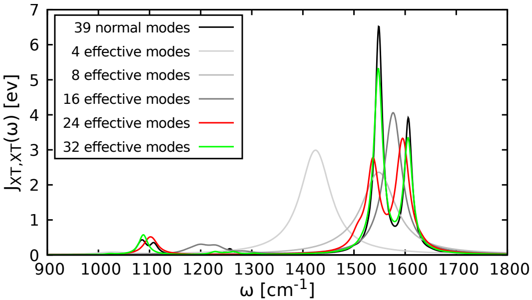

- generalized effective-mode construction for correlated *e-ph* interactions
- SDs shown for two-site (dimer) system
- convergence at intermediate order
- transferable to larger aggregate stacks

Popp, Polkehn, Tamura, Burghardt, to be submitted

Vibronic Coupling Model – 13 States, 196 modes

$$\hat{H} = \hat{H}^{\text{on-site}} + \hat{H}^{\text{coup}} + \hat{H}^{\text{e-ph}}$$

$$\hat{H}^{\text{coupl}} = j \sum_{n=1}^{N} |\text{XT}_n\rangle\langle\text{XT}_{n+1}| + \kappa_1 \sum_{n=1}^{N-1} |\text{XT}_n\rangle\langle\text{CTX}_{n+1,n}| + \kappa_2 \sum_{n=1}^{N-1} |\text{XT}_n\rangle\langle\text{CTX}_{n,n+1}| + h.c.$$

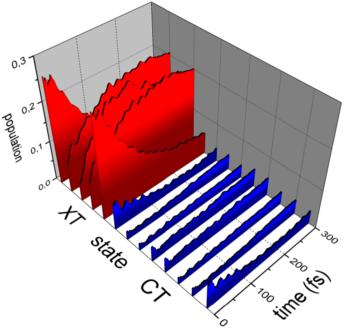

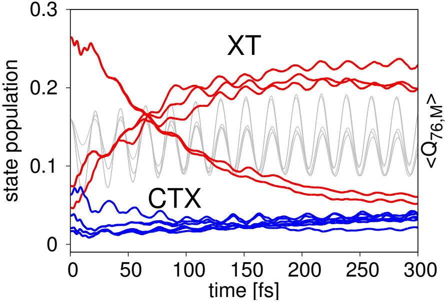

- two diabatization schemes Tamura, JPCA, 120, 9341 (2016), Blancafort, Voityuk, JCP 140, 095102 (2014)
- pronounced oscillatory signature in all state populations

Collective Electronic & Vibrational Dynamics

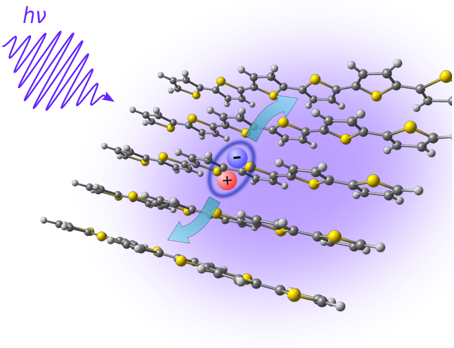

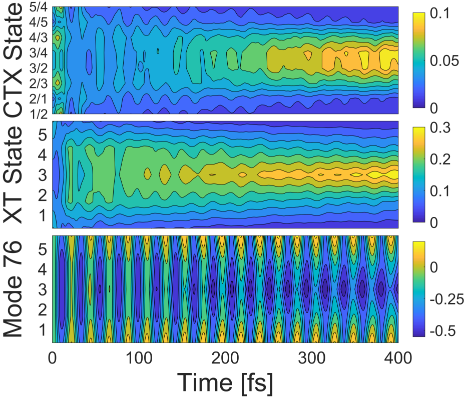

- coherent formation of XT/CTX quasi-stationary polaron species
- high-frequency normal modes of OT fragments are evolving in phase
- amplification (& synchronization) of vibronic effects due to delocalization
- similar observations for intra-chain dynamics Binder et al., Phys. Rev. Lett. 120, 227401 (2018)

Collective Electronic & Vibrational Dynamics

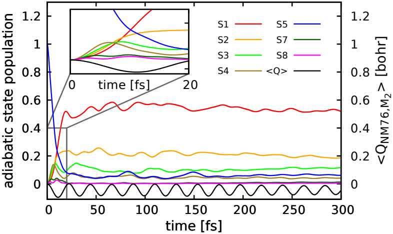

ultrafast internal conversion

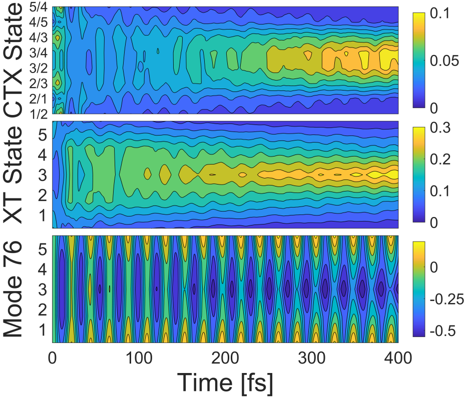

- coherent formation of XT/CTX quasi-stationary polaron species
- high-frequency normal modes of OT fragments are evolving in phase
- amplification of vibronic effects due to exciton delocalization
- similar observations for intra-chain dynamics Binder et al., Phys. Rev. Lett. 120, 227401 (2018)

Do CTX States Affect Interfacial Charge Generation?

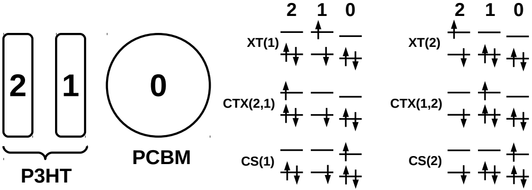

	XT(1)	XT(2)	CTX(2,1)	CTX(1,2)	CS(1)	CS(2)
XT(1)	0.100	0.100	0.357	0.139	0.200	0.007
XT(2)		0.100	0.139	0.357	0.014	0.013
CTX(2,1)			0.280	0.001	0.005	0.002
CTX(1,2)				0.230	0.019	0.165
CS(1)					0.000	0.102
CS(2)						0.140

Polkehn, Tamura, Burghardt, J. Phys. B, 51, 014003 (2018)

- CTX-to-CS transfer can circumvent interfacial XT-to-CS transfer step
- here: parameter determination via diabatization by projection onto reference wavefunctions Tamura, JPCA 120, 9341 2016, Polkehn, Tamura, Burghardt, J. Phys. B, 51, 014003 (2018)

Interfacial Charge Separation in the Presence of CTX States

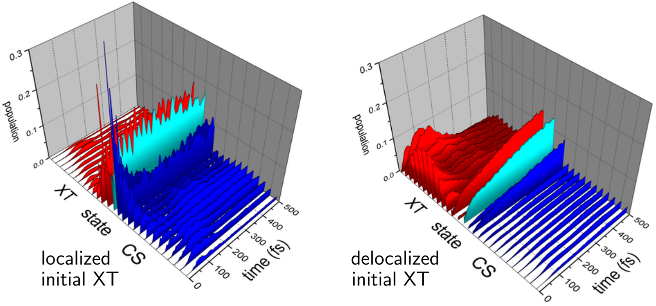

- CTX (turquoise) states emerge prominently as additional energetic traps
- ML-MCTDH calculations up to 182 states and 112 modes
- for a single CTX state: CS formation slightly reduced
- for larger models (50/182 states): reduction of CS yield is significant
- results depend in a sensitive fashion upon energetics and electronic couplings

Polkehn, Tamura, Burghardt, J. Phys. B, Special Issue "Light Energy Conversion, Light Harvesting", 51, 014003 (2018).

P3HT/PCBM Model Including CTX States

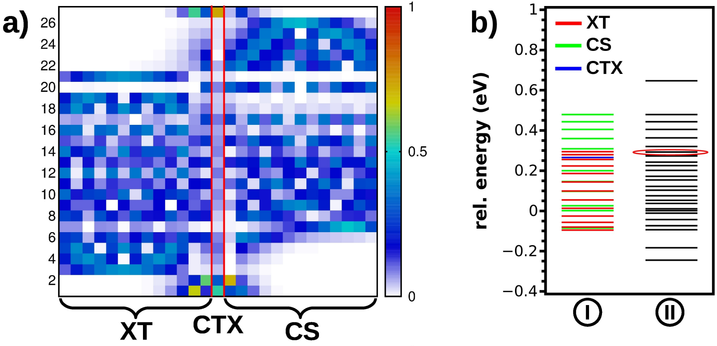

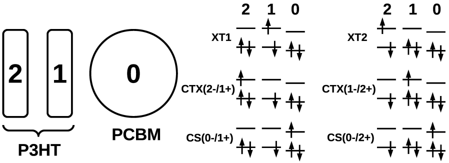

- 182 states/112 modes
- OT charge transfer excitons open new pathways for carrier formation
- but also act as energetic traps

Polkehn, Tamura, Burghardt, J. Phys. B, 51, 014003 (2018)

Summary

1. Molecular-Level Approach to Organic Photovoltaics
   - e-h lattice model: highlights fragment properties + molecular packing
   - extensions to conical intersections, multi-exciton states[1] etc.
   - accurate *on-the-fly* dynamics remains highly challenging

---

[1] See our work on singlet fission: Tamura, Huix-Rotllant, Burghardt, Olivier, Beljonne, Phys. Rev. Lett. 115, 107401 (2015)

Summary

❶ Molecular-Level Approach to Organic Photovoltaics

- *e-h* lattice model: highlights fragment properties + molecular packing
- extensions to conical intersections, multi-exciton states[1] etc.
- accurate *on-the-fly* dynamics remains highly challenging

❷ Coherent Exciton Dynamics & Role of Nano-Morphology

- ultrafast ($\sim$ 50-100 fs) coherent initial charge separation
- Coulomb barrier to free carrier formation reduced in regioregular domains
- elementary exciton-polaron migration step is coherent

---

[1] See our work on singlet fission: Tamura, Huix-Rotllant, Burghardt, Olivier, Beljonne, Phys. Rev. Lett. 115, 107401 (2015)

Summary

❶ Molecular-Level Approach to Organic Photovoltaics

- e-h lattice model: highlights fragment properties + molecular packing
- extensions to conical intersections, multi-exciton states[1] etc.
- accurate *on-the-fly* dynamics remains highly challenging

❷ Coherent Exciton Dynamics & Role of Nano-Morphology

- ultrafast ($\sim$ 50-100 fs) coherent initial charge separation
- Coulomb barrier to free carrier formation reduced in regioregular domains
- elementary exciton-polaron migration step is coherent

❸ Manifestations of Electron-Phonon Coupling

- e-ph coupling drives exciton dissociation *via* nonadiabatic transitions
- high-frequency modes give rise to exciton (and charge) trapping
- low-frequency torsional fluctuations induce exciton migration

---

[1] See our work on singlet fission: Tamura, Huix-Rotllant, Burghardt, Olivier, Beljonne, Phys. Rev. Lett. 115, 107401 (2015)

Summary

❶ Molecular-Level Approach to Organic Photovoltaics

- e-h lattice model: highlights fragment properties + molecular packing
- extensions to conical intersections, multi-exciton states[1] etc.
- accurate *on-the-fly* dynamics remains highly challenging

❷ Coherent Exciton Dynamics & Role of Nano-Morphology

- ultrafast ($\sim$ 50-100 fs) coherent initial charge separation
- Coulomb barrier to free carrier formation reduced in regioregular domains
- elementary exciton-polaron migration step is coherent

❸ Manifestations of Electron-Phonon Coupling

- e-ph coupling drives exciton dissociation *via* nonadiabatic transitions
- high-frequency modes give rise to exciton (and charge) trapping
- low-frequency torsional fluctuations induce exciton migration

---

[1] See our work on singlet fission: Tamura, Huix-Rotllant, Burghardt, Olivier, Beljonne, Phys. Rev. Lett. 115, 107401 (2015)

Acknowledgments & Collaborations

Group Frankfurt:

- M. Polkehn
- P. Eisenbrandt
- R. Binder
- J. von Cosel
- K. Falahati
- T. Ma
- W. Popp
- M. Bonfanti
- K. Schwinn

Former members:

- J. Wahl
- M. Huix-Rotllant

Collaborations:

- H. Tamura (Tokyo, Japan)
- W. H. Miller, S. Cotton, R. Liang (Berkeley)
- K. H. Hughes (Bangor, UK)
- R. Martinazzo (Milano, Italy)
- H. Lischka, A. Aquino (TTU, USA)
- F. Plasser (Vienna, Austria)
- D. Lauvergnat (Orsay, France)
- S. Haacke, S. Méry (Strasbourg, France)
- G. D'Avino (Institut Néel, Grenoble)
- G. A. Worth (London, UK)
- A. Panda (IIT Guwahati, India)
- D. Beljonne, Y. Olivier (Mons, Belgium)

Thanks to: DFG / ANR (France) for financial support

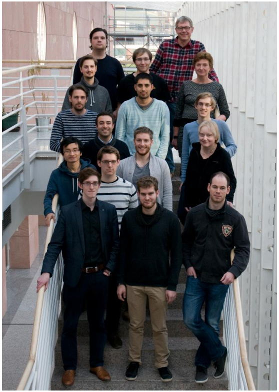

ϱ Theoretical Chemistry
of Complex Systems

AK Burghardt

MCTDH – Equations of Motion

Coupled system of coefficient equations and low-dimensional non-linear equations for single-particle functions (SPFs) $\varphi^{(\kappa)}$:

coefficients:
$$i\frac{dA_J}{dt} = \sum_L \langle \Phi_J | H | \Phi_L \rangle A_L$$

SPFs:
$$i\frac{\partial \varphi^{(\kappa)}}{\partial t} = \left(\hat{1} - \hat{P}^{(\kappa)} \right) \left[\rho^{(\kappa)} \right]^{-1} \hat{H}^{(\kappa)} \varphi^{(\kappa)}$$

Meyer, Manthe, Cederbaum, CPL **165**, 73 (1990), Beck et al., Phys. Rep. **324**, 1 (2000)

- $\hat{P}^{(\kappa)} = \sum_j |\varphi_j^{(\kappa)}\rangle\langle\varphi_j^{(\kappa)}|$ is the time-dependent projector on the κth subspace
- $\hat{H}_{ij}^{(\kappa)} = \langle \psi_i^{(\kappa)} | \hat{H} | \psi_j^{(\kappa)} \rangle$ are mean-field Hamiltonian matrix elements
- $\rho_{ij}^{(\kappa)} = \langle \psi_i^{(\kappa)} | \psi_j^{(\kappa)} \rangle$ are reduced density matrix elements in the κth subspace
- recent approaches to “repair” singularity problem ($[\rho^{(\kappa)}]^{-1}$)

Manthe, J. Chem. Phys. **142**, 244109 (2015), Wang, Meier, J. Chem. Phys. **148**, 124105 (2018),
Lubich, Appl. Math. Res. Express 2, 311-328 (2015), Kloss, Burghardt, Lubich. J. Chem. Phys., 146, 174107 (2017)

Improved Semiclassical Methods: SQC/MM (T=0K)

SQC/MM – single trajectory

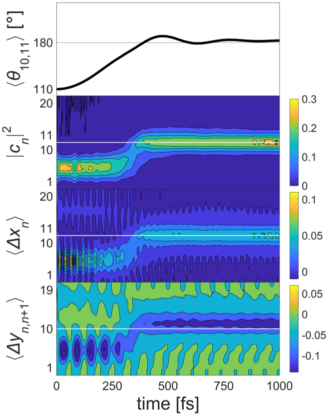

SQC/MM – Wigner average

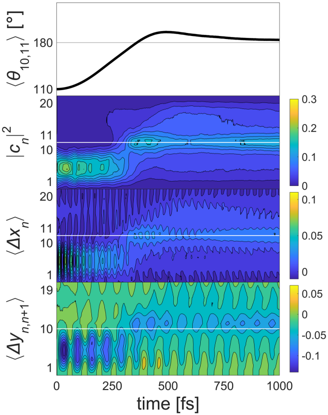

- SQC/MM = Symmetrical Quasi-Classical / Meyer-Miller model
- single-trajectory result close to MCTDH, but Wigner average “fuzzy”

Liang, Cotton, Binder, Hegger, Burghardt, Miller, J. Chem. Phys., 149, 044101 (2018)

Ehrenfest/Langevin dynamics (T=0K)

Ehrenfest – single trajectory

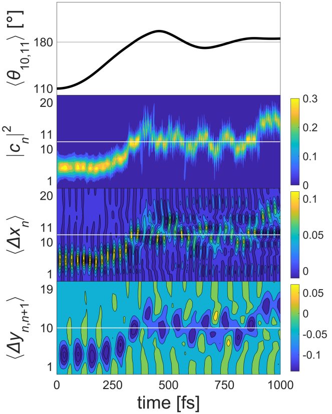

Ehrenfest – Wigner average

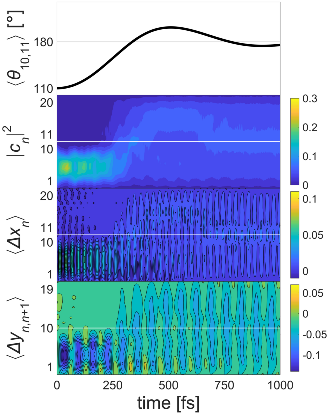

- single-trajectory dynamics exhibits fluctuations
- Wigner average "fuzzy" – due to Wigner sampling of high-frequency modes

Liang, Cotton, Binder, Hegger, Burghardt, Miller, J. Chem. Phys., in press (2018)

Adiabatic Populations (T=0K)

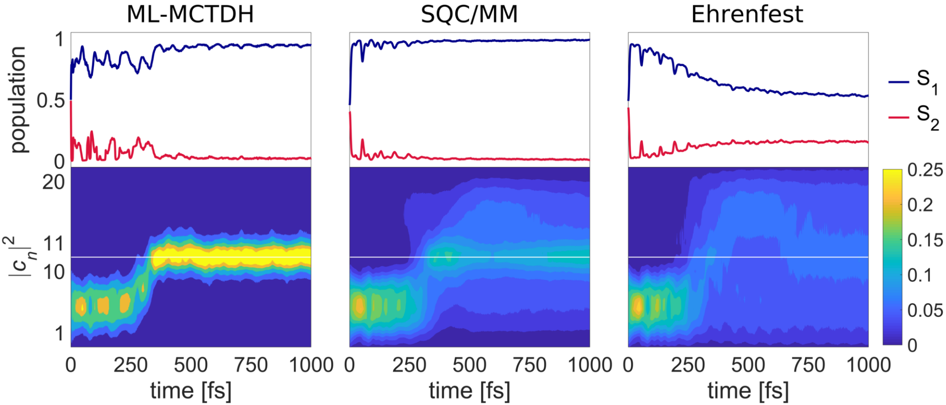

- SQC/MM reproduces the adiabatic populations quite accurately
- Ehrenfest shows severe shortcomings (related to detailed-balance problem)
- both methods incur problems due to ZPE of high-frequency modes

Liang, Cotton, Binder, Hegger, Burghardt, Miller, J. Chem. Phys., in press (2018)

Initial vs. Final States: Absorption Spectra

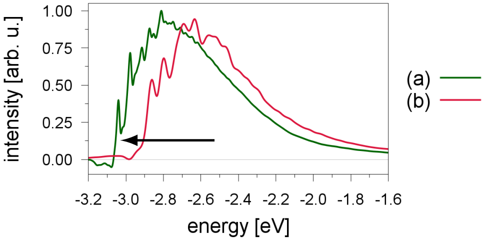

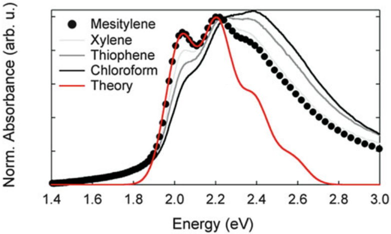

Tremel, Ludwigs, Adv. Polym. Sci. 265, 39 (2014)

- spectra calculated from Fourier transform of $C(t) = \langle \psi(0) | \psi(t) \rangle$:
  (a) full 20-mer system: torsionally relaxed, stationary state
  (b) left-localized 10-mer fragment for initial defect structure
  (a) $\longleftarrow$ (b): downhill energy transfer
- dominant vibronic signature of ring-breathing mode

OT System – FFT

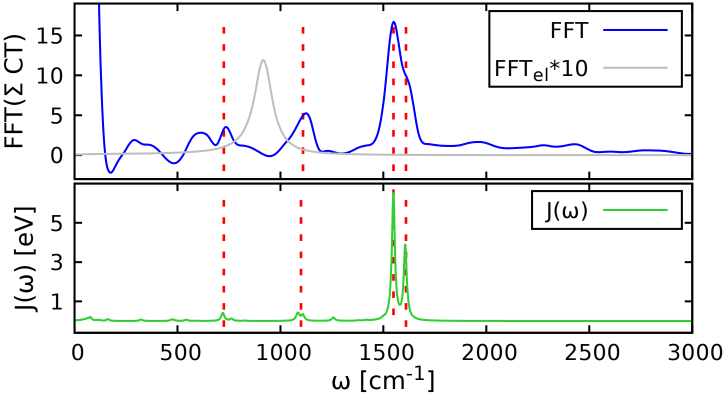

- Fourier transform and spectral density – OT

Free Carrier Generation, Cont'd

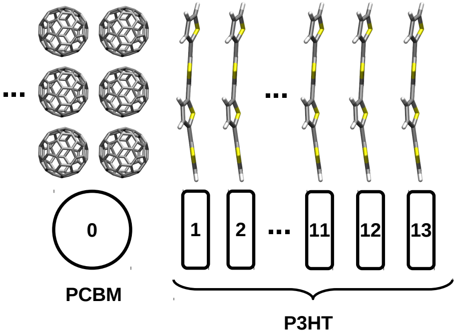

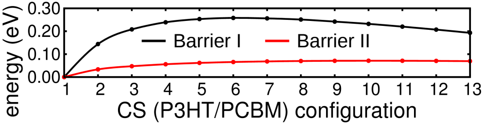

Tamura, Burghardt, JACS (Communication) 135, 16364 (2013)

Huix-Rotllant, Tamura, Burghardt, J. Phys. Chem. Lett., 6, 1702 (2015)

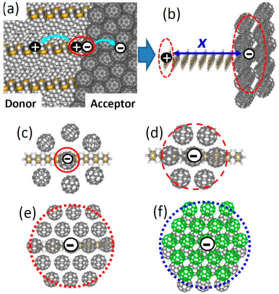

factors favoring ultrafast *e*-*h* separation:

- electron delocalization over fullerene aggregates: strong decrease of barrier
- hole delocalization on oligothiophenes
- XT delocalization in H-aggregate donor
- exciton (XT) excess energy: "Hot CT" mechanism

Highly Ordered DA Assemblies: Liquid Crystalline Material

collaboration with S. Haacke, S. Méry (Strasbourg), G. D'Avino (Grenoble)

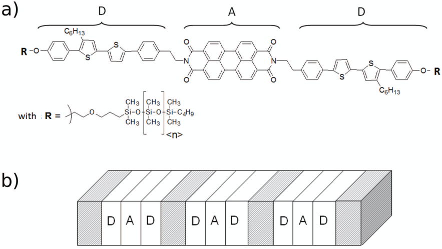

Roland, Ramirez, Léonard et al., PCCP, 14, 273 (2012)

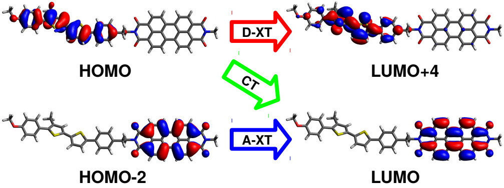

Wenzel, Dreuw, Burghardt, PCCP, 15, 11704 (2013)

- competing ultrafast energy transfer (EET) and charge transfer (CT) processes
- in chloroform: EET in 130 fs, followed by CT in 2.7 ps
- in liquid crystalline phase: CT in 60 fs!
- relatively fast recombination (50 ps) – material doesn't really work well . . .

What is Happening in the First-Generation Material?

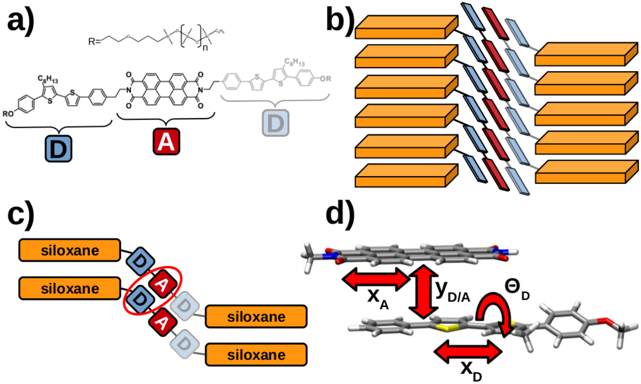

Polkehn et al., J. Phys. Chem. Lett., 7, 1327 (2016)

- first-generation material: liquid crystalline smectic mesophase
- idea: D/A stacks serve as “quantum wells” for carrier transport
- much faster charge transfer in film than solution ($\sim$50 fs vs. $\sim$3 ps)
- calculations suggest unexpected inter-chain D-A interactions

Liquid Crystalline Phase – Energetics

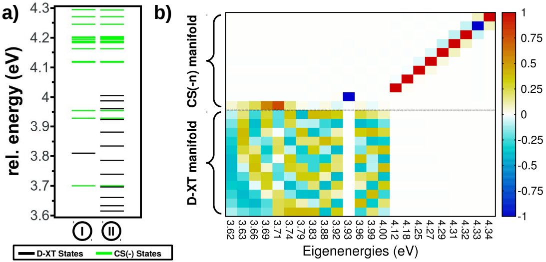

- energetics at Franck-Condon geometry
- state mixing: excitonic manifold and CS(-1) state
- but higher charge separated states barely accessible

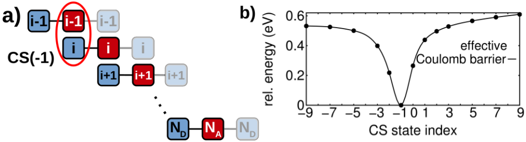

- on-site energies computed from ADC(2) and TDDFT
- internal field: 20 V/μm
- CS(-1) state strongly stabilized

Polkehn, Tamura, Eisenbrandt, Haacke, Méry, Burghardt, J. Phys. Chem. Lett., 7, 1327 (2016)

Liquid Crystalline Phase – Dynamics

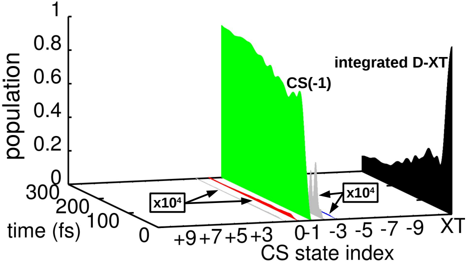

Polkehn et al., JPCL (2016)

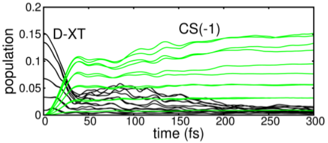

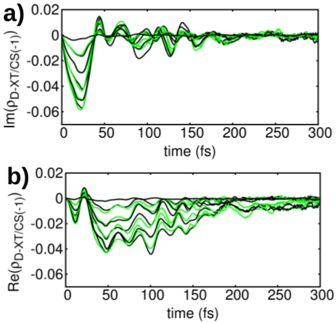

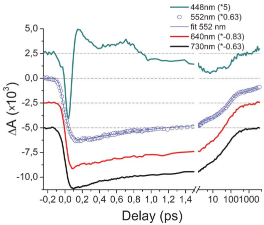

Roland et al., PCCP (2012)

- transition to CS(-1) states (∼50 fs) explains transient absorption experiments (Haacke)
- ML-MCTDH simulations for 156 states/48 modes

Second Generation Material: Zipper-like Molecular Packing

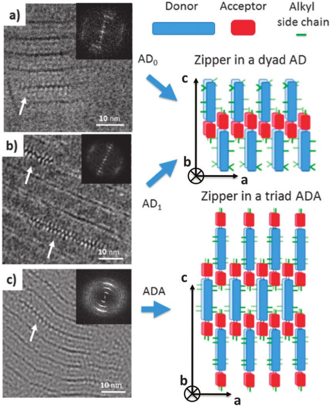

Biniek et al., J. Mater. Chem. C 3, 3342 (2015)

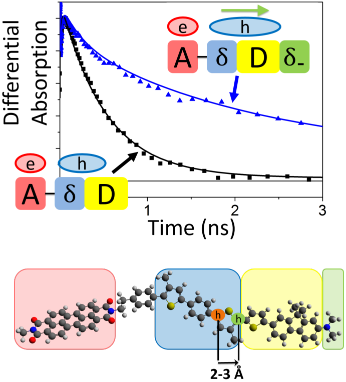

Liu, Eisenbrandt et al., PCCP 18, 18536 (2016)

- tunable donor species: alternating thiophene/fluorene/benzothiadiazole units; electrodeficient bridge to the perylene acceptor – chemical design!
- organization in lamellae (both DA and ADA – but not DAD)
- comparatively slow CT formation (tens of ps) - and less recombination

Second Generation Material: In Progress . . .

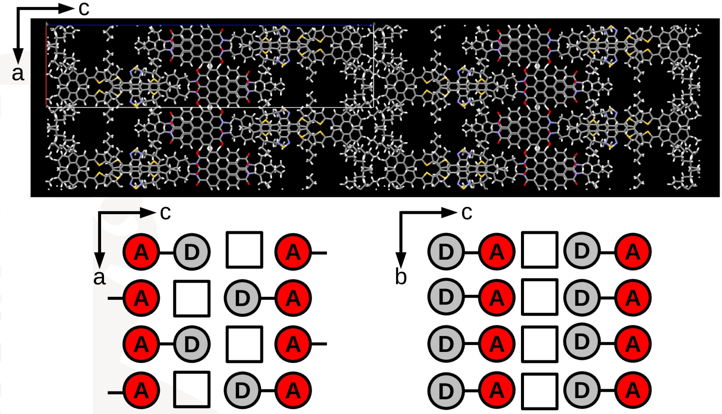

- coarse-grained model for Kinetic Monte Carlo (KMC) simulations
- microelectrostatics calculations (collaboration with G. D'Avino, Grenoble)
- multi-scale modeling needed!

Second Generation Material: In Progress . . .

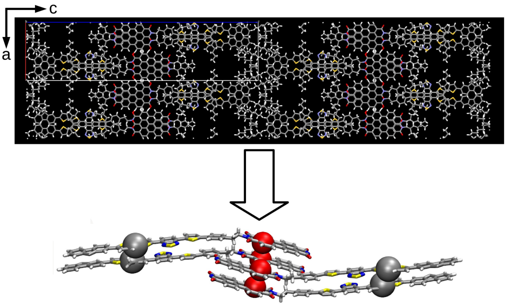

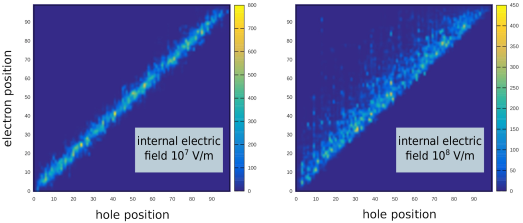

- transport mainly through perylene stacks
- highly efficient e transport: $\mu_{-} = 0.016$ cm^2/Vs
- far less efficient h transport: $\mu_{+} = 1.3 \cdot 10^{-6}$ cm^2/Vs

- KMC simulations using microelectrostatics (D'Avino)
- simulations predict so far $\mu_{-}/\mu_{+} \sim 10$ (Schwinn et al.)
- quantum transport analysis in progress
- spectroscopy: intermediate species (triplet, bipolaron, excimer?) (Haacke & coll.)

Singlet Fission: Route To Carrier Multiplication

(collaboration with H. Tamura (Sendai/Tokyo), D. Beljonne (Mons))

$$\boxed{\text{XT} \longrightarrow {}^1(\text{TT}) \longrightarrow \text{T}_1 + \text{T}_2 \text{ (spin conserving)}}$$

possibly overcome Shockley-Queisser limit

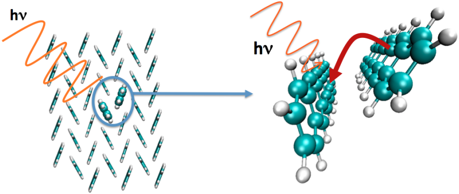

http://sites.lsa.umich.edu/zimmerman-lab/wp-content/uploads/sites/52/2014/03

- driving force $\Delta E_{\mathrm{XT-TT}} < 0$ doesn't explain the whole picture
- possible involvement of intermediate CT states (superexchange)
- vastly different time scales for different materials

- discovered in 1965: anthracene
- reviews by Smith & Michl, Annu. Rev. Phys. Chem. 2013, 64, 361, Chem. Rev. 110, 6891 (2010)

Molecular Packing: Energetics & Electronic Couplings

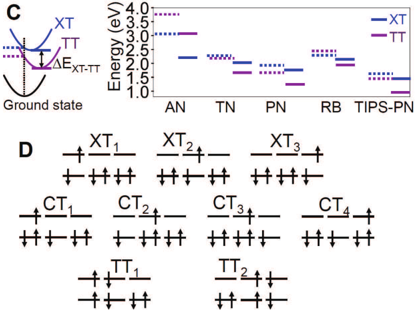

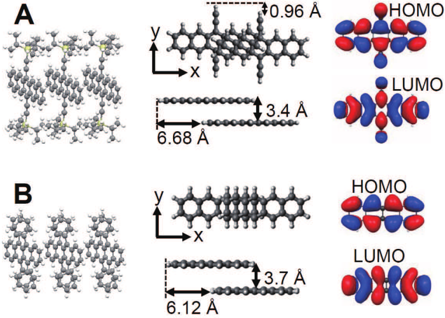

- energetics of acene series (C)
- trimer model: 9 states (D)

- TIPS-pentacene (A): slip-stacked
- rubrene (B): C_{2h} symmetric

Electronic coupling @ equilib. non-zero for TIPS-pentacene but vanishing for rubrene!
(MRMP2 calculations for dimers, el. couplings via diabatization protocol)

Tamura, Huix-Rotllant, Burghardt, Olivier, Beljonne, Phys. Rev. Lett., 115, 107401 (2015)

TIPS-Pentacene: Ultrafast Singlet Fission

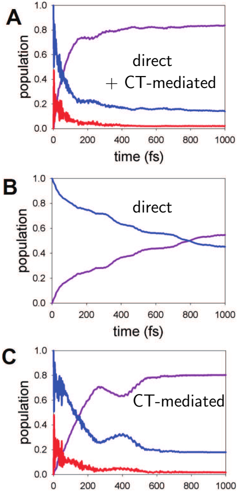

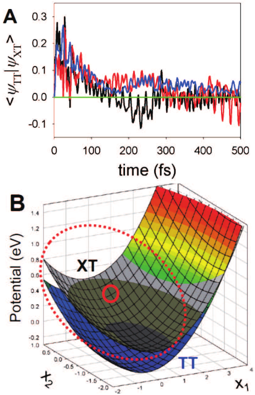

- ultrafast, coherent SF
- slip-stacked geometry: avoided crossing
- interfering direct and CT-mediated pathways (electronic coupling via CT's dominates)
- vibrational coherence effectively transferred between XT and TT states (see $\langle \psi_{\mathrm{TT}} | \psi_{\mathrm{XT}} \rangle$)

  Musser et al., Nature Phys. 11, 352 (2015)
- MRMP2 calculations + diabatization

Tamura, Huix-Rotllant, Burghardt, Olivier, Beljonne, Phys. Rev. Lett., 115, 107401 (2015)

Rubrene: Thermally Activated Singlet Fission

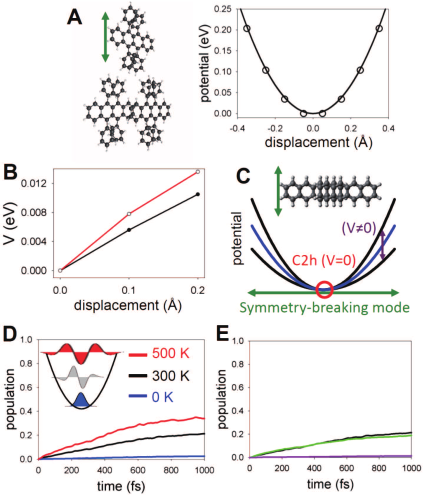

- driving force slightly exergonic (like tetracene), but thermally activated SF (picosecond scale)
- C_{2h} crystal geometry: electronic coupling vanishes – conical intersection
- electronic couplings depend on symmetry-breaking coordinate: $V(X) = \lambda X$, $\lambda \sim 10^{-3}$ eV
- slow, incoherent dynamics
- key influence of molecular packing

Tamura, Huix-Rotllant, Burghardt, Olivier, Beljonne, Phys. Rev. Lett., 115, 107401 (2015)

ML-MCTDH: Example

Binder, Polkehn, Ma, Burghardt, Chem. Phys. 482, 16 (2017)

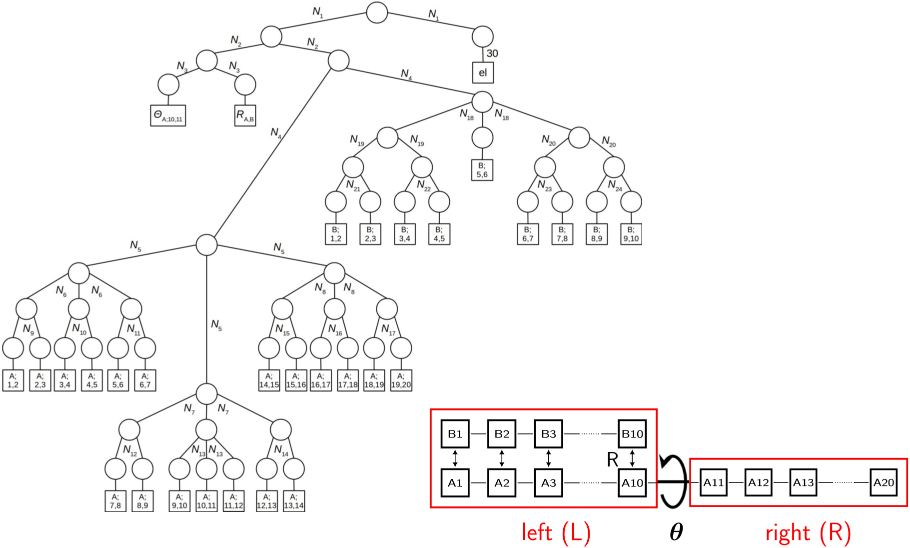

Exciton-Polaron Dynamics: Adiabatic Picture

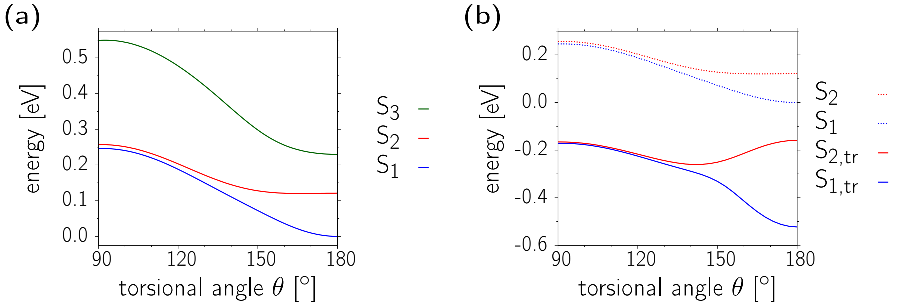

- dynamics is essentially happening on coupled S_1/S_2 surfaces
- effective torsion potentials including stabilization due to trapping $(S_{1,\mathrm{tr}}/S_{2,\mathrm{tr}})$[1]
- initial left/right localized state = superposition of S_1/S_2
- energy loss due to external bath acting on torsional mode
- exciton-polaron trapping persists at all stages of the dynamics

---

[1] i.e., "polaron transformed" potentials

Quantum Dynamics: 20-Site J-Aggregate with Central Torsion

C-C inter-monomer mode + local C=C + torsion + bath

C-C inter-monomer + torsion + bath

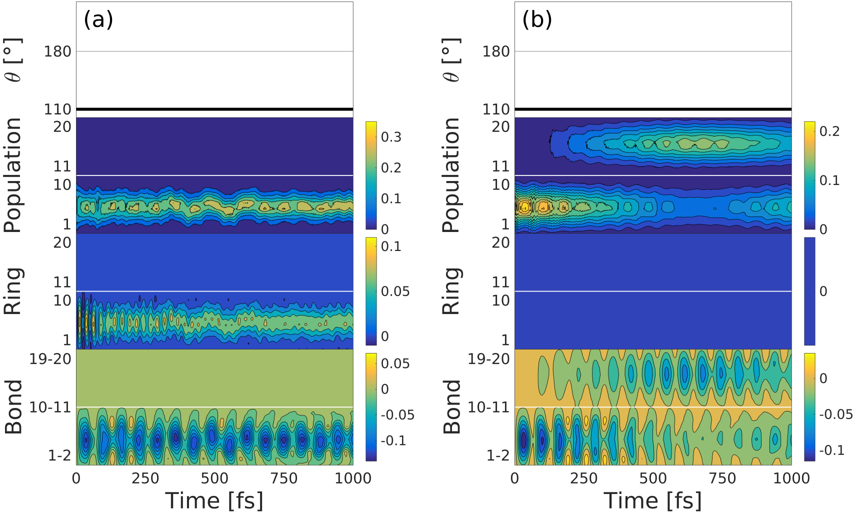

Interfacial Charge Separation in the Presence of CTX States

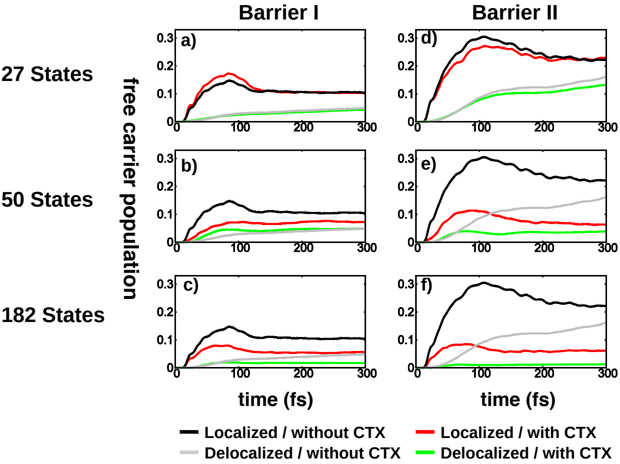

- time-dependent free carrier populations

Polkehn, Tamura, Burghardt, J. Phys. B, Special Issue "Light Energy Conversion, Light Harvesting", submitted (2017)

System-Bath Models

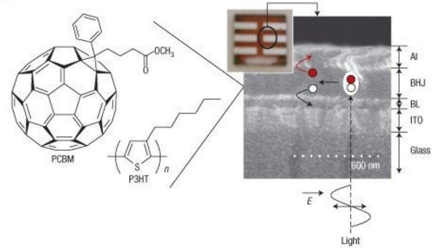

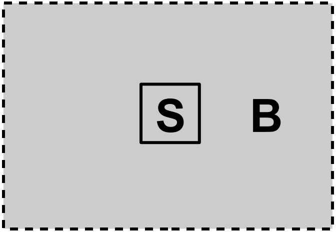

S region: e.g., electronic degrees of freedom (electron-hole states)

B region: all vibrations (phonons) mapped to harmonic oscillator model

$$\hat{H}_B + \hat{H}_{SB} = \sum_n \frac{1}{2}(\hat{p}_n^2 + \frac{1}{2}\omega_n^2 \hat{x}_n^2) + \hat{s}\sum_n c_n \hat{x}_n$$

$$\boxed{J(\omega) = \pi/2 \sum_n c_n^2/\omega_n \delta(\omega - \omega_n)}$$

spectral density

Spectral Densities from Electronic Structure Calculations$^{(*)}$

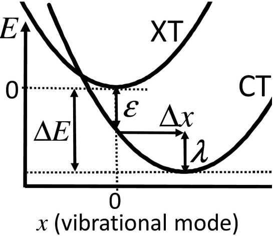

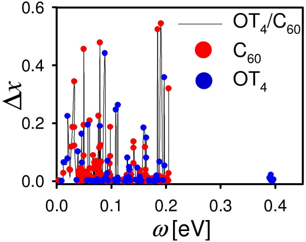

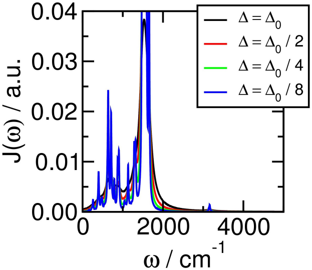

$$J(\omega) = \frac{\pi}{2} \sum_n^N \frac{c_n^2}{\omega_n} \delta(\omega - \omega_n) \simeq \frac{\pi}{2} \sum_n^N \frac{c_n^2}{\pi} \frac{\Delta}{(\omega - \omega_n)^2 + \Delta^2}$$

Tamura, Martinazzo, Ruckenbauer, Burghardt, J. Chem. Phys., 137, 22A540 (2012)

$^{(*)}$NB. Alternatively: obtain SD's from correlation functions (MD, CPMD, . . .)